AD NUMBER

AD864968

NEW LIMITATION CHANGE

TO

Approved for public release, distribution unlimited

FROM

Distribution authorized to U.S. Gov't. agencies and their contractors; Administrative/Operational Use; Dec 1969. Other requests shall be referred to Air Force Materialsw Lab., Attn: MAMC, Wright-Patterson AFB, OH 45433.

AUTHORITY

USAFML ltr, 29 Mar 1972

AFML-TR-69-84
PART II. VOLUME II

STABILITY CHARACTERIZATION OF REFRACTORY MATERIALS UNDER HIGH VELOCITY ATMOSPHERIC FLIGHT CONDITIONS

PART II. VOLUME II: FACILITIES AND TECHNIQUES EMPLOYED FOR COLD GAS/HOT WALL TESTS

LARRY KAUFMAN
HARVEY NESOR
ManLabs, Inc.

TECHNICAL REPORT AFML-TR-69-84, PART II, VOLUME II

DECEMBER 1969

AIR FORCE MATERIALS LABORATORY
AIR FORCE SYSTEMS COMMAND
WRIGHT-PATTERSON AIR FORCE BASE, OHIO

NOTICE

When Government drawings, specifications, or other data are used for any purpose other than in connection with a definitely related Government procurement operations, the United States Government thereby incurs no responsibility nor any obligation whatsoever; and the fact that the Government may have formulated, furnished, or in any way supplied the said drawings, specifications, or other data, is not to be regarded by implication or otherwise as in any manner licensing the holder or any other person or corporation, or conveying any rights or permission to manufacture, use, or sell any patented invention that may in any way be related hereto.

This document is subject to special export controls and each transmittal to foreign governments or foreign nationals may be made only with prior approval of the Air Force Materials Laboratory, MAMC, Wright-Patterson Air Force Base, Ohio 45433.

The distribution of this report is limited for the protection of technology relating to critical materials restricted by the Export Control Act.

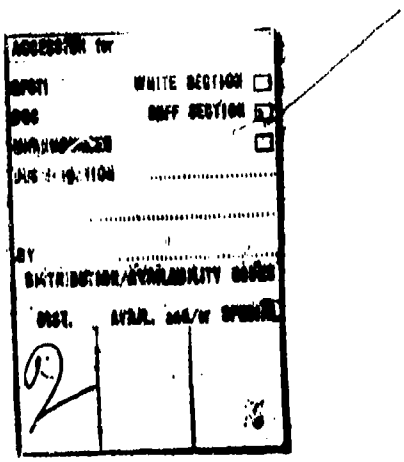

Copies of this report should not be returned unless return is required by security considerations, contractual obligations, or notice on a specific document.

700 - January 1970 - CO455 - 105-2335

STABILITY CHARACTERIZATION OF REFRACTORY MATERIALS UNDER HIGH VELOCITY ATMOSPHERIC FLIGHT CONDITIONS

PART II. VOLUME II: FACILITIES AND TECHNIQUES EMPLOYED FOR COLD GAS/HOT WALL TESTS

LARRY KAUFMAN

HARVEY NESOR

FOREWORD

This report was prepared by ManLabs, Inc. under Project 7312, "Metal Surface Deterioration and Protection", Task 731201, "Metal Surface Protection", and Project 7350, "Refractory Inorganic Nonmetallic Materials", Task Nos. 735001, "Refractory Inorganic Nonmetallic Materials: Nongraphitic", and 735002, "Refractory Inorganic Nonmetallic Materials: Graphitic", under AF33(615)-3859 and was administered by the Metals and Ceramics Divisions of the Air Force Materials Laboratory, Air Force Systems Command, with J. D. Latva, J. Krochmal and N. M. Geyer acting as project engineers.

This report covers the period from April 1966 to July 1969.

ManLabs personnel participating in this study included L. Kaufman, H. Nesor, H. Bernstein, E. Peters, J.R. Baron, G. Stepakoff, R. Pober, R. Hopper, R. Yeaton, S. Wallerstein, E. Sybicki, J. Davis, K. Meaney, K. Ross, J. Dudley, E. Offner, A. Macey, A. Silverman and A. Constantino.

The manuscript of this report was released by the authors in September 1969 for publication. This technical report has been reviewed and is approved.

W. G. Ramke
Chief, Ceramics and Graphite Branch
Metals and Ceramics Division
Air Force Materials Laboratory

The following reports will be issued under this contract.

Part/Volume	
I-I	Summary of Results
II-I	Facilities and Techniques Employed for Characterization of Candidate Materials
II-II	Facilities and Techniques Employed for Cold Gas/Hot Wall Tests
II-III	Facilities and Techniques Employed for Hot Gas/Cold Wall Tests
III-I	Experimental Results of Low Velocity Cold Gas/Hot Wall Tests
III-II	Experimental Results of High Velocity Cold Gas/Hot Wall Tests
III-III	Experimental Results of High Velocity Hot Gas/Cold Wall Tests
IV-I	Theoretical Correlation of Material Performance with Stream Conditions
IV-II	Calculation of the General Surface Reaction Problem

ABSTRACT

The oxidation of refractory borides, graphites and JT composites, hypereutectic carbide-graphite composites, refractory metals, coated refractory metals, metal oxide composites, and iridium coated graphites in air over a wide range of conditions was investigated over the spectrum of conditions encountered during reentry or high velocity atmospheric flight as well as those employed in conventional furnace tests. Elucidation of the relationship between hot gas/cold wall (HG/CW) and cold gas/hot wall (CG/HW) surface effects in terms of heat and mass transfer rates at high temperatures is a principal goal. The present report deals with facilities and techniques employed for performing low velocity CG/HW tests. These techniques include low velocity tests in resistance heated tube furnaces, low-velocity tests of inductively heated samples, and high velocity tests of inductively heated samples. Oxidation exposures performed by these techniques span the temperature range between 1000° and 4200°F at flow rates between 0.2 ft/sec and 300 ft/sec. Measurements of the temperature gradients through thin oxide films (10-60 mils thick) indicate that large differences up to 800°F are noted near 3500°F. These results have special significance with regard to interpretation of oxidation measurements and behavior.

TABLE OF CONTENTS

LIST OF ILLUSTRATIONS

LIST OF TABLES

BLANK PAGE

I. INTRODUCTION AND SUMMARY

A. Introduction

The response of refractory materials to high temperature oxidizing conditions imposed by furnace heating has been observed to differ markedly from the behavior in arc plasma "reentry simulators." The former evaluations are normally performed for long times at fixed temperatures and slow gas flows with well-defined solid/gas-reactant/product chemistry. The latter on the other hand are usually carried out under high velocity gas-flow conditions in which the energy flux rather than the temperature is defined and significant shear forces can be encountered. Consequently, the differences in philosophy, observables, and techniques used in the "material centered" regime and the "environment centered, reentry simulation" area differ so significantly as to render correlation of material responses at high and low speeds difficult if not impossible in many cases. Under these circumstances, expeditious utilization of the vast background of information available in either area for optimum matching of existing material systems with specific missions or prediction and synthesis of advanced material systems to meet requirements of projected missions is sharply curtailed.

In order to progress toward the elimination of this gap, an integrated study of the response of refractory materials to oxidation in air over a wide range of time, gas velocity, temperature and pressure has been designed and implemented. This interdisciplinary study spans the heat flux and boundary-layer-shear spectrum of conditions encountered during high-velocity atmospheric flight as well as conditions normally employed in conventional materials centered investigations. In this context, significant efforts have been directed toward elucidating the relationship between hot gas/cold wall (HG/CW) and cold gas/hot wall (CG/HW) surface effects in terms of heat and mass transfer rates at high temperatures, so that full utilization of both types of experimental data can be made.

The principal goal of this study is the coupling of the material-centered and environment-centered philosophies in order to gain a better insight into systems behavior under high-speed atmospheric flight conditions. This coupling function has been provided by an interdisciplinary panel composed of scientists representing the component philosophies. The coupling framework consists of an intimate mixture of theoretical and experimental studies specifically designed to overlap temperature/energy and pressure/velocity conditions. This overlap has provided a means for the evaluation of test techniques and the performance of specific materials systems under a wide range of flight conditions. In addition, it provides a base for developing an integrated theory or modus operandi capable of translating reentry systems

requirements such as velocity, altitude, configuration, and life time into requisite materials properties as vaporization rates, oxidation kinetics, density, etc., over a wide range of conditions.

The correlation of heat flux, stagnation enthalpy, Mach Number, stagnation pressure, and specimen geometry with surface temperature through the utilization of thermodynamic, thermal and radiational properties of the material and environmental systems used in this study was of prime importance in defining the conditions for overlap between materials-centered and environment-centered tests.

Significant practical as well as fundamental progress along the above mentioned lines necessitated evaluation of refractory material systems which exhibit varying gradations of stability above 2700°F. Emphasis has been placed on candidates for 3400°F to 6000°F exploitation. Thus, borides, carbides, boride-graphite composites (JTA), JT composites, carbide-graphite composites, pyrolytic and bulk graphite, PT graphite, coated refractory metals/alloys, oxide-metal composites, oxidation-resistant refractory metal alloys, and iridium-coated graphites were considered. Similarly, a range of test facilities and techniques including oxygen pickup measurements, cold sample hot gas, and hot sample cold gas devices at low velocities, as well as different arc plasma facilities capable of covering the 50-2500 BTU/ft^{2}sec flux range under conditions equivalent to speeds up to Mach 12 at altitudes up to 200,000 ft were employed. Stagnation pressures covered the range between 0.001 and 10 atmospheres. Splash and pipe tests were performed in order to evaluate the effects of aerodynamic shear. Based on the present results, this range of heat flux and stagnation enthalpy produced surface temperatures between 2000°F and 6500°F.

B. Summary

This report describes the facilities and techniques employed in the Cold Gas/Hot Wall tests performed at ManLabs, Arthur D. Little, and Lockheed M/S Co. Low velocity testing was performed at ManLabs, Inc. under the direction of H. Nesor. Air flowing at 0.9 to 9.0 ft/sec was employed in resistance heated tube furnaces at temperatures between 1000°F and 4200°F. Exposure times ranging from five minutes up to four hours were used to evaluate the behavior of the candidate materials. Post exposure metallographic examination of samples disclosed the extent of oxidation. Temperature measurement within the tube furnaces was carried out by means of optical brightness and two color pyrometry and checked by measurements of the melting temperature of several materials.

Low velocity tests of inductively heated samples were performed at Arthur D. Little under the direction of J.B. Berkowitz-Mattuck. Tests were performed in oxygen-helium mixtures at flow rates of 0.2 ft/sec. and oxygen partial pressures of 0.013 to 0.20 atm. Oxidation behavior was continuously monitored by measuring the rate at which oxygen was removed from the stream for times up to one hour. These measurements were complimented by measurements of CO and CO_2 formation. Post exposure metallographic measurements were employed to check and supplement the gas analysis data.

Optical brightness measurements were employed to measure the surface temperature.

High velocity Cold Gas/Hot Wall tests of inductively heated samples were performed at Lockheed M/S Co. under the direction of Roger Perkins. These exposures were performed between 2000°F and 4500°F at flow rates between 10 and 300 ft/sec. for times up to one hour. Post exposure metallographic analysis was employed to measure the extent of oxidation. Temperature measurements of the surface by means of optical brightness and two-color pyrometry was employed to evaluate the spectral emittance of the oxidizing surface. In addition, temperature gradients through the oxide were measured by monitoring the temperature at the root of internal holes drilled to within 100 mils of the surface. Temperature gradients of the order of 800°F were observed for thin oxide films. In these cases, the surface temperature was lower than the internal temperature. These gradients exercise an important degree of control over the oxidation behavior and the observed kinetics. With induction heating, the metallic substrate is heated directly by coupling with the electromagnetic field. The nonconducting oxide scale, however, does not couple with the field and is heated indirectly by conduction from the heated substrate. The surface is cooled by radiation and convection. This leads to an inverse gradient in which the temperature at the metal/oxide interface is higher than that at the oxide/air interface. As the oxide thickens with time, the resistance to heat transfer is increased. If the substrate temperature is held constant, surface temperature will decrease. If the surface temperature is held constant, the substrate temperature must be increased to overcome the added resistance to heat flow.

The importance of this aspect of materials behavior depends upon the rate-controlling factor in the oxidation process. Since the surface temperature is measured and controlled in most tests of materials, oxidation data will be accurate only if surface temperature controls the reaction rate. If the substrate or interface temperature is rate controlling, however, the measured rate of oxidation will be too high or too low, depending on the method of heating used in conducting the tests. If the substrate is heated by induction or direct resistance, it will be hotter than the surface. If the surface is heated by radiation, the substrate may be cooler or at the same temperature, depending on heat losses to supporting devices or structures. In most gas torch or plasma tests, the substrate will be cooler than the surface. Only in furnace tests where the sample is brought to a uniform temperature throughout, will the surface and substrate be at the same temperature.

II. LOW VELOCITY TESTS IN RESISTANCE HEATED TUBE FURNACES

Cold Gas/Hot Wall furnace tests between 1000°F and 4200°F were performed in flowing air at one atmosphere for times varying between five minutes and four hours using flow rates ranging from 0.9 to 9.0 ft/sec. Moreover, cyclic heating and cooling exposures were also carried out for candidate materials which exhibit protective coatings that form during oxidation. The extent to which oxidation takes place during the exposure is determined by post oxidation metallography. The procedure for performing these tests consists of heating samples by radiation from a zirconia tube which is in turn heated by radiation from a carbon tube resistance furnace. A schematic diagram of the apparatus is shown in Figure 1. The specimen is heated from room temperature in argon to the desired temperature prior to introduction of flowing air. The heat-up times are from 15 to 45 minutes depending on test temperature. Next, flowing air displaces the argon and is passed through the zirconia tube during the oxidation exposure at rates of 10-80 ft^3/hr in the smaller furnaces and 40-80 ft^3/hr in the larger furnaces. These flow rates correspond to linear velocities of 0.9 to 7.2 ft/sec and 0.9 to 1.8 ft/sec in the small and large size furnaces, respectively. Cylindrical specimens are mounted on zirconia pads with the cylindrical axis normal to the direction of air flow. After the oxidation period is completed, the air is displaced by argon and the sample is cooled.

Cooling time to 400°F is 60 minutes in the small furnace and 90 minutes in the large furnace. Cyclic exposures requiring multiple cycles are run sequentially with a heat up, oxidation hold, cool down, heat up, oxidation hold, cool down, etc. Subsequent to cool down and removal from the furnace, the sample is photographed and sectioned for metallic analysis.

In the present study, two furnace sizes have been employed. The smaller furnace contains a 7/8 inch diameter x 12 inches long zirconia tube into which the specimen is placed on zirconia pads. The larger furnace contains a 2 inch inside diameter by 36 inches long zirconia tube muffle. The smaller furnace is employed in the oxidation of 1/2 inch diameter by 1/2 inch long specimens. The larger furnace is used for one inch samples. The furnaces are operated at constant power for the selected temperature which can be maintained within 20°F. The power is controlled manually by either a saturable reactor or an SCR power supply. At the temperatures of most of the tests, there is about a seven-fold increase in the absolute temperature of the gas, so the velocity is 7-50 ft/sec.

The specimen surface temperature is measured and recorded continuously by means of Rockwell (formerly Latronics) and Milletron two-color pyrometers. These instruments are calibrated against a calibrated tungsten lamp certified by the National Bureau of Standards. The color temperature of the tungsten filament is obtained from the brightness temperature which in turn is directly related to the operating current of the lamp. The color temperature-brightness temperature relation is based on the emittance of tungsten at 0.665 and 0.467 microns. The two-color

pyrometer was also compared with a brightness pyrometer using a blackbody target in a carbon block and in ZrO_2 brick. These comparisons were performed in the 3/4 inch ID tube furnace over the temperature range between 2700° to 4000°F. The agreement between instruments was found to be within 20°F. The two-color pyrometers were also employed to measure the melting points of iron, platinum, platinum-10% rhodium, platinum-40% rhodium, Al_2O_3, Hf-20Ta-2Zr, and Hf-20Ta-2Mo in the small oxidation furnace, with argon flowing under conditions which were exactly the same as employed in the oxidation exposures. The results obtained in these experiments followed by the literature values in parentheses are: iron-2880°F (2797°F), platinum - 3272°F (3218°F), platinum - 10% rhodium - 3353°F (3295°F), platinum - 40% rhodium - 3533°F (3525°F), Al_2O_3 - 3705°F (3695°F), Hf-20Ta-2Zr - 3920°F (3860°F), Hf-20Ta-2Mo - 3857°F (3860°F). Figures 2-4 show post exposure photomicrographs of test $HfB_{2.1}$(A-2), OX-268 after 60 minutes. Measurements of the length and diameter prior to and after exposure indicated a longitudinal conversion depth (diboride to oxide) of 16 mils and a transverse conversion depth of 16 mils. In cases where different conversion depths are measured, the maximum value is employed in characterizing the behavior. This technique has been employed successfully in measuring the oxidation behavior of refractory oxidation resistant materials (1-4)*

*Underscored numbers in parentheses indicate references given at the end of this report.

III. LOW VELOCITY TESTS OF INDUCTIVELY HEATED SAMPLES

Oxidation tests were performed on samples which were inductively heated between 2900° and 4000°F during exposure to flowing mixtures of oxygen and helium. Flow rates of 0.2 ft/sec at oxygen partial pressures of 0.013 to 0.20 atmospheres and total pressures of one atmosphere were employed. Oxidation behavior was monitored by continuously measuring the rate at which oxygen was removed from the stream. The measurements of oxygen pickup rate were complemented by continuous measurements of CO and CO_2 formation in the case of the graphite composites. These continuous measurements were complemented by post exposure metallographic analysis of the samples. Changes of oxygen concentration in the gas stream resulting from reaction with the samples, were followed continuously by means of a thermal conductivity method (1), (5). As shown schematically in Figure 5, the gas stream flows through a thermal conductivity cell (TC-I) containing a thermistor bead detector and over the heated sample, where some of the oxygen is lost by reaction. The oxygen depleted stream passes through a second thermal conductivity cell (TC-II) similar to the first. The two cells, TC-I and TC-II, form two arms of a Wheatstone bridge, whose recorded output at any time is thus directly proportional to the rate of reaction of the sample at that time. The recorded rate curve is automatically integrated to give net extent of reaction over a given time period.

The experimental method described above is actually sensitive to changes in the composition of any permanent gases in the reacting stream. For silicides and borides, oxygen depletion alone affects the recorded signal. For carbides (6,7), or carbon containing materials in general, oxidation results not only in the depletion of oxygen, but also in the introduction of CO and CO_2 into the gas stream. The modified experimental method described below was therefore employed for the graphite composites.

After reaction, the gas stream depleted in oxygen, but enriched in CO and CO_2, is passed through a weighed Ascarite bulb to remove the CO_2. The remaining mixture of CO, O_2 and He is then passed through TC-II. The resultant recorder output is proportional to the difference between the net rate of oxygen consumption and the rate of formation of CO. Finally, upon leaving TC-II, the CO in the gas stream is oxidized over cupric oxide powder at 500°C, and the CO_2 produced is collected in a second weighed Ascarite bulb.

All samples were degassed in pure helium at the planned experimental temperature for 30-60 minutes prior to oxidation. Brightness temperatures were measured optically at $\lambda = 0.65\mu$ and corrected to true temperatures by employing an emittance at $\lambda = 0.65\mu$.

The kinetic data obtained from the thermal conductivity method; that is, grams of oxygen consumed, W, as a function of time, t, for a given temperature, and initial surface area, A_o, were analyzed by

plotting the quantity $(W/A_o)^2$ vs. time, t. This procedure afforded a linear relationship as shown in Figure 6 indicating parabolic oxidation behavior. This relationship is described analytically as

$$\left(\frac{W}{A_o}\right)^2 = k_{pp}t \tag{1}$$

where k_{pp} is the parabolic rate constant. In principle, the quantity A_o is also a function of time and the data analysis should account for this variation. In practice, this correction is second order for most of the conditions employed in this study.

The relation between oxygen consumption and conversion of the diboride to oxide has been discussed previously (2). Briefly, in the case of diborides which can oxidize according to Eq. 2 where Me = Zr, Hf, the parabolic rate constant for oxygen consumption, $k_{pp}(g^2/cm^4\text{-min})$ is related to the parabolic rate constant for alloy consumption, $k_{px}(cm^2/min)$ by Eq. 3

$$MeB_2(s) + \frac{5}{2}\ O_2(g) \rightarrow MeO_2(s) + B_2O_3\ (s \text{ or } \ell) \tag{2}$$

$$k_{pp} = (k_{px})\ (\rho^2_{MeB_2})\ \frac{25M_O^2}{M^2_{MeB_2}} \tag{3}$$

where ρ_{MeB_2} is the density of the metal diboride and M_{MeB_2} is the molecular weight of MeB_2 and M_O is the molecular weight of oxygen. Thus, for both HfB_2 and ZrB_2

$$k_{pp}\ (gms^2/cm^4min) = 20\,k_{px}(cm^2/min) \tag{4}$$

Thus, Eqs. 2 through 4 imply that

$$d^2 = k_{px}t \tag{5}$$

where d is the average depth of boride converted to oxide in a time, t. If d is in mils and t in hours, then

$$d^2\ (mils^2) = 4.8 \times 10^5\, k_{pp}\ (gm^2/cm^4min)\ t\ (hr) \tag{6}$$

The quantity d is measured directly by the metallographic techniques or calculated from the k_{pp} values via these equations.

For example, Figures 7 and 8 show longitudinal and transverse sections of a metal rich hafnium diboride sample after a one hour exposure at 3360°F in which a parabolic rate constant of 5.0×10^{-4} was determined. Substitution of this value into Eq. 6 yields a conversion depth of 15.8 mils as compared with values of 15.7 and 15.8 mils determined metallographically. In this sense, the post-mortem measurements provided a check of the thermal conductivity (oxygen pickup) measurements.

For carbon-containing samples, S, the signal from the thermal conductivity cell, is given by:

$$S = k_1 (p_{O_2, TC-I} - p_{O_2, TC-II}) - k_2 p_{CO, TC-II} \quad (7)$$

where k_1 and k_2 are calibration constants, $(p_{O_2, TC-I} - p_{O_2, TC-II})$ is the oxygen consumed in units of pressure and $p_{CO, TC-II}$ is the pressure of CO (g) in the second thermal conductivity cell. To an excellent approximation, the thermal conductivity method is equally sensitive to CO and O_2, and therefore $k_1 = k_2$. If w_{O_2} is the mass per unit time of oxygen consumed to form solid and volatile oxide products, we have from the ideal gas law:

$$(p_{O_2, TC-I} - p_{O_2, TC-II}) = \frac{w_{O_2}}{M_{O_2}} \left(\frac{RT}{\phi}\right) \quad (8)$$

where M_{O_2} is the molecular weight of oxygen, and ϕ is the volume flow rate. The oxygen consumed per unit time, w_{O_2}, can be written as the sum of the weight of oxygen consumed in formation of CO_2 and CO, and the weight of oxygen consumed, w_O sol. information of solid oxide products. The quantity w_O sol. reflects both oxides that remain on the sample surface (e.g., ZrO_2) and those that volatilize at the experimental temperature, but condense on the cool walls of the reaction chamber (e.g., B_2O_3). Finally

$$w_{O_2} = \frac{M_{O_2}}{M_{CO_2}} w_{CO_2} + \frac{M_O}{M_{CO}} w_{CO} + w_O \text{ sol.} \quad (9)$$

where w_{CO_2} and w_{CO} are the weight of CO_2 and CO formed per unit time.

Finally, substituting Eqs. 8 and 9 into Eq. 7 yields the following expression for the recorded signal:

$$S = \frac{RT}{\phi} k_1 \left[\frac{w_{CO_2}}{M_{CO_2}} + \frac{w_{O', sol.}}{M_{O_2}} - \frac{w_{CO}}{2M_{CO}} \right] \quad (10)$$

The calibration constant k_1 was determined by measuring the signal obtained upon introduction of known pulsed quantities of O_2 and CO into the apparatus (8).

A recorder tracing for the oxidation of an Ir-Rh-Re sample is reproduced in Figure 9. The rate of oxygen pickup by the reacting sample in g/min of oxygen consumed, is given as a function of time. Similar curves were obtained in every experiment. The rate of oxidation was observed to rapidly reach a maximum level and then to remain linear for time periods that varied from 5-30 minutes. Subsequently, the rate began to drop with time in the stepwise manner illustrated in Figure 9. Since the oxides of the platinum metals are known to be highly volatile at the temperatures of the present series of experiments, the rate of oxidation is expected to be independent of time. Consequently, the cause of the observed decrease in rate is presently unknown. However, even the initial linear rate is low compared to the true surface reaction controlled rate. Consequently, it is possible that the apparent drop in rate with time is due to changes in the pattern of flow of metal oxides away from the surface and oxygen towards the surface. The observed rate of oxygen consumption was employed to compute the rate of metal consumption based on a fixed oxide stoichiometry. The results were checked by post exposure metallography.

IV. HIGH VELOCITY TESTS OF INDUCTIVELY HEATED SAMPLES

High velocity Cold Gas/Hot Wall, CG/HW, oxidation exposures were performed at Lockheed Missile/Space Company in order to extend the furnace air oxidation tests to speeds of 300 ft/sec and provide comparison data for the Mach 0.3 exposures to be performed in the Model 500 facility at Avco/SSD. These exposures were carried out by inductively heating a one half inch diameter rod of the specimen material under high flow conditions.

A. Test Equipment and Procedures

The schematic diagram shown in Figure 10 illustrates the general configuration and arrangement of equipment employed for these tests. Basically, the apparatus is a vertical wind tunnel in which the test specimen is heated inductively. A quartz tube, 1.5-in. I.D. by 20-in. long, is used as the test section. It is attached to a Buffalo Forge Company, size 2, 250cfm Type R.E. exhauster driven by a 2 HP motor at 3500 rpm. An adjustable damper was installed in the exhaust line from the test section (inlet to fan) to regulate gas velocity. It was found that air flow rates from 0 to 250 fps could be established in the test section (1.5-inch I.D. x 20-inch quartz tube). The maximum rate (250 fps) is slightly less than the design maximum (300 fps) calculated from blower size and system geometry. This most likely is due to high frictional losses resulting from screening of the fan inlet to prevent ingestion of hot specimens and bending of the exhaust at right angles to the inlet stream. Flow rates are measured with a water manometer and a static pressure tube located 4-in. below the test section inlet.

A cylindrical test specimen, 0.5-inch diameter by 1 to 1.5-inch long, is supported on an adjustable stinger at the midpoint of the test section. Initially, as shown in Figure 10, a hollow stinger was used to permit measurement of true temperature (blackbody hole) and temperature gradients of the samples. In most tests, however, a water-cooled copper tube was used for the stinger and support to prevent reaction with the test sample at high temperature. Temperature of the top surface is measured by sighting on a front surface mirror mounted above the venturi inlet. Test specimens are heated by induction from an externally wound coil connected to either a 30 KW - 10000 cps Tocco motor generator set or a 23 KVA - 475 KC Lepel high frequency generator. The low frequency power supply was used for high conductivity (metallic-type samples) and the h.f. unit was used for high resistance materials (graphite, SiC, etc). The Lepel unit and power supply arrangement are shown in Figure 11. Temperatures up to 5000°F were obtained at flow rates up to 150 fps. A thin gold coating is applied to the inside of the quartz tube for radiation shielding.

The test procedure consisted first of aligning the specimen, mirrors, and optical pyrometers and establishing the required gas velocity in cold flow. Full power was then applied to the induction coil and the sample heated to the test temperature in 15 to 30 sec. Power input is cut back to the control level and air flow adjusted as needed to compensate for gas heating effects. The time for start of test is taken at the instant the desired run temperature is reached. Power input is adjusted and controlled manually throughout the test. Control to within + 20°F of test temperature was maintained at all temperatures from 2000 to 4000°F. The true surface temperature was

measured with a Milletron two color pyrometer using the assumption that all materials (except graphite) behaved as a grey body (color temperature equals true temperature). For tests with graphite, color temperature corrections were used. The apparent surface (brightness) temperature was measured at a wavelength 0.65μ with a Pyrometer Instrument Corp. precision micro-optical pyrometer. Both instruments were calibrated periodically with a certified NBS tungsten filament lamp. The two temperature measurements, true (T) and brightness (θ), were used to calculate the normal spectral emittance (ϵ_{N_λ}) according to Wein's law:

$$\ln \epsilon_{N\lambda} = C\lambda^{-1}\left(\frac{1}{T} - \frac{1}{\theta}\right)$$

where T and θ = °Rankine
C = 25880°R microns
λ = 0.65 microns

On completion of the test, the power was turned off and the cold air flow maintained at full level to quench the sample. The time for end of test was taken as the time of power shut down.

B. Development of Test Capabilities

1. Flow Field and Specimen Configuration

Calculations indicate that turbulent flow will exist in the test section at gas velocities of 5 fps or higher. Based on air at 68°F, the Reynolds number at 160 ft/sec flow in a 1.5 inch diam. tube is 25,000. The transition to turbulent flow in a straight circular pipe begins at 2100°F, and flow will always be turbulent with a Reynolds number above 4000. With turbulent flow, the velocity distribution across the tube will be more uniform. The average velocity is about 80% of the maximum gas velocity, compared with a 50% value for laminar flow conditions. The existence of turbulent flow will create more severe environmental conditions for oxidation tests in high velocity air. Also, it will result in high rates of heat transfer from the sample to the gas. This, in some cases, may limit the operating temperatures that can be obtained with the existing power supply.

The nature of the flow field and its effect on surface recession rates at various points on a sample was studied using graphite test cylinders. As shown in Figure 12, the flow separates at the edges of a flat faced cylinder. This produces a wide free shear layer with eddies near the surface. The flow over hemispherical end specimens is more uniform. The free shear layer is thin and shows no abrupt changes or eddies along the surface. The effects on surface recession of graphite at 3400°F are shown in Figure 13. Flow separation with flat faced specimens results in low recession rates on the diameter near the leading edge. High recession rates near the trailing edge indicates a tendency for the flow to reattach with considerable turbulence in the wake region. This results in the generation of a tear drop

shape with wide variations in surface recession rates at different locations on the sample. Hemispherical end specimens recede more uniformly as a result of the smooth flow field and tend to form bullet (ogive) configurations. Surface recession rates on the diameter decrease gradually from top to bottom. Surprisingly, the surface recession rate of the stagnation region was about the same for both types of specimens (2 mil/sec).

Materials with high surface recession rates presented a major problem in testing due to the shape changes that occurred. Tests were conducted with 0.5-inch diam. by 1 to 1.5-inch long cylinders of Speer 710 Graphite to establish the optimum specimen configuration. It was found that a conical tip with a 30° angle was a relatively stable configuration in this test apparatus at gas velocities of 50 to 250 fps. This is the limiting configuration that other shapes tend to approach (Figure 13). Conical tipped samples yielded accurate surface recession data over a wide range of temperatures and flow rate. A 30° cone tip was selected as standard geometry for all tests on graphite and other high recession rate materials. The experimental work leading to the development of this sample is discussed in detail in Part III, Volume II of this series of reports.

2. Coil Design and Coupling Studies

A series of tests were made with the Lepel 475 KC, 23 KVA high frequency power supply to establish the maximum temperature of test for various materials as a function of air flow ratio. A 1-1/2 inch ID by 8-1/2 turn coil was used without a susceptor or radiation shields. The sample was heated to the maximum temperature possible (full power on) in very slowly moving air (~1 fps). The air flow was maintained at a level sufficient to prevent smoke or fumes from rising up the flow tube and fogging the mirrors used for temperature measurement. Readings were taken on the top surface with the Milletron two color pyrometer. Air flow was increased to 50, 75, 100, 125 and 150 fps, and the maximum steady state top surface temperature attained at full power output was measured. The results are compiled in Table 1 and are shown graphically in Figure 14. The effect of gas velocity on cooling is quite striking, particularly on the borides and the Hf-Ta alloys where 900° and 500°F drops in temperature, respectively, were observed with air flowing at 150 fps. These operational capabilities are considerably below the desired test ranges for the experimental program. They represent the maximum capability with the existing design. Possibilities for increasing these capabilities include the use of a different power supply and the use of radiation shields as reduction of flow tube and coil diameter to achieve better coupling. Tests indicate that boride samples and Hf-19Ta-2Mo heat much better with a lower frequency power supply. The coupling studies were repeated using a Tocco 10 KC 30 KW motor generator set. The inside surface of the flow tube was gold plated to provide a radiation shield. Results of tests are summarized in Table 2. At 150

fps, temperatures of 2950°F (Hf-Ta) and 3200°F (ZrB_2) were reached. For the Hf-Ta alloy, this is lower than the maximum temperature reached with the Lepel 475 kc high frequency generator. However, for the ZrB_2 sample, coupling with the 10 kc Tocco generator was better, and higher temperatures than those previously attained were reached. In both cases, however, the maximum temperatures at high gas velocity is low compared with the desired test range (3400°-3800°F).

Consideration was given to the use of focused induction coils to improve coupling and increase maximum operating temperatures. Three different types of coils were evaluated in an effort to improve coupling in the induction heating of small samples:

a. Straight cylindrical
b. Hourglass shaped (focusing)
c. Short cylindrical with flat pancake end coils (focusing)

All tests were made with a 10 kc, 30 kw Tocco motor generator induction unit. The type (a) coil was found to be least effective and the type (c) coil was found to give best results. Results are summarized in Figure 15.

With straight cylindrical coils, length-to-diameter ratio of the coil and number of turns were varied to determine the effect on coupling. Best results were obtained by having as many turns as possible of the smallest possible diameter within a length of about 2 to 3 inches. The minimum coil diameter was dictated by the outside diameter of the flow tube (1-3/4 inch). The maximum number of turns in a given length was determined by the size of copper tube used to wind the coil. Tubing smaller than 1/4-inch O.D. could not be used due to the inability to circulate enough cooling water through the coil. Even with 1/4-inch copper, the coil water temperature at full power was 150 to 180°F, which is near the cut off limit for the generator. (Occasional shutdowns due to high water temperature have occurred in the course of full power runs). Much better cooling was obtained with 5/16 or 3/8-inch copper tube; however, in these cases, the number of turns is too small for good coupling with small samples. Best results with cylindrical coils were obtained with a 1-3/4 I.D., 12-turn coil (1/4-inch copper tube) about 4 to 5 inches long. With this coil, Hf-Ta-Mo samples on ZrO_2 supports could be heated to 3400°F in slowly moving air and to 3180°F in air at 50 fps.

A significant improvement in coupling was obtained by winding the coil with an hourglass shape to focus or concentrate the lines of flux in a central region around the test sample. A central turn was wound to the minimum diameter (1-1/2 inches) and each successive turn in either direction was wound to a larger diameter than the turn before. The best coil had 15 turns, 7 turns on each side of the central turn with a smoothly graded diameter from 1-1/2 to 3-inches I.D. With this coil, the Hf-Ta-Mo (on ZrO_2) was heated to 3300°F in air flowing at 150 fps. This is a gain of 400°F over the best straight cylindrical coil. The ZrB_2 sample (on ZrO_2) was held at 3600°F in air at 150 fps. This was also a gain of 400°F.

Experiments with the hourglass coil indicated that still further improvements were possible by compressing the total length of the coil relative to the length of the specimen. The ultimate in compression was obtained by winding a short cylindrical coil with two flat pancake focusing coils, one at each end. The cylindrical portion was wound with 2 to 9 turns at 1-1/2 inches I.D., and each pancake coil had four turns of increasing diameter to a maximum of 5-inches O.D. Tests with these coils gave best results with 4 to 5 turns in the cylindrical section. Temperatures above 3400°F and 3600°F at 150 fps were obtained for Hf-Ta-Mo and ZrB_2, respectively.

An unusual effect was observed in testing of the KT-SiC cylinders. Using a 475 KC Lepel high-frequency generator, the samples were effectively coupled with a 1-1/2-inch I.D. by 8-1/2 turn coil. On reaching a temperature of 2550°F, the coupling improved by several orders of magnitude and temperature increased rapidly to beyond 4000°F with no increase in power output. This effect is shown by the data plotted in Figure 16. The steady state value of temperature was measured for each level of control current. On reaching 2550°F, the sample heated rapidly and the control current was reduced from 1.075 amp to 0.325 amp to hold a temperature of 2650°F. From this temperature up, the sample behaved like a metallic susceptor. On cooling below 2550°F, the sample reverted to the poor susceptance characteristic of conventional SiC. The effect was completely reversible and showed little hysteresis. As shown in Figure 16, the effect was not observed with commercial SiC tube used for Globar heaters. This material was a poor susceptor and could not be heated above 2950° with the full output (3 amp) of the generator.

It has been reported that KT-SiC contains about 9% free silicon. Eutectic melting occurs in the Si-SiC system at 2552°F. It seems clear that the effect is related to melting of silicon in the "alloy". Metallographic examination revealed each grain of SiC to be surrounded by a thin film of silicon after heating near 2550°F. Before heating, no intergranual films were detected. Illustrations of the structural changes during the 2550°F coupling transition in KT-SiC are shown in Figure 17. The formation of a continuous intergranular network of Si after heating above the melting point of Si is clearly indicated. The photographs also show composition gradients and some evidence of precipitation withir the SiC phase after heating to high temperature. This behavior indicates some solid solubility of Si in SiC. The phase diagram, however, indicates little, if any, solid solubility.

A second coupling transition was found for KT-SiC at about 4000°F. This one appears to be related to the phase transformation (hexagonal to cubic) at 4000°F in SiC. Cubic SiC (>4000°F) is an excellent susceptor and good coupling is attained. A sample was heated to 4700°F in air flowing at 150 fps at a fraction of the available power. This temperature is about 150°F below the dissociation temperature for SiC. Oxidation was so rapid that combustion almost was self sustaining. A sheet of flame and smoke extended several inches beyond the trailing end of the sample. The appearance of the sample after test is shown in Figure 18. The sample fused with the ZrO_2 support rod. Crystals of ZrSi were found precipitated from a melt of a Si-Zr alloy that had penetrated completely throughout the sample (top to bottom and side to side).

A white coating of ZrO_2 had formed on the outer surface of the piece. The oxidation rate seemed to be lower in the Zr-rich lower portion of the sample, even though this region was at a higher temperature than the top surface. Surface recession of the top was surprisingly low. These findings are in contrast to the behavior of KT-SiC(E-14) in the Air Oxidation Tests where rapid oxidation is observed above 3500°F and the Arc Plasma Tests where rapid oxidation is observed above 4000°F. The enhanced behavior may be due to the pick up of zirconium by the KT-SiC.

3. Temperature Measurement and Control

Temperature distributions over the surface and through the cross section of test cylinders in static and flowing air were studied to establish methods for accurate measurement and control of temperature and to define more clearly the limitations of cold-flow tests with induction-heated samples.

Initial tests were conducted with graphite cylinders 0.5-inch diameter by 1.5-inch long with a hemispherical leading edge. The temperature at the stagnation point and at the root of a blackbody hole drilled axially in from the base of the sample was measured simultaneously with micro-optical pyrometers (0.65μ). In static tests, the distance between the root of the blackbody hole and the stagnation point was varied to determine the temperature gradient, if any, through the wall. As shown in Figure 19, little if any gradient existed with a wall thickness of 0.1 inch. The apparent surface temperature was lower than the hole temperature due to emittance effects. Normal spectral emittance was estimated to range between 0.7 and 0.8 over the temperature range of 2400° to 3000°F. This is in reasonable agreement with published data on the emittance of graphite. When the wall thickness was increased to 0.3 or 0.4 inch, a noticeable temperature gradient was observed. The surface temperature was 100° to 200°F lower for a given hole temperature compared with 0.1-inch wall specimens. The gradient was larger at the higher temperature where the rate of heat loss by radiation becomes pronounced. Flowing air past the specimen at 150 fps had a pronounced cooling effect on the surface in the low temperature range where heat loss by conduction was large compared with the loss of radiation. Surface temperature decreased an additional 300°F in the range 2200° to 2600°F. At high temperature, an additional 100°F drop was observed in flow.

Studies using graphite as a model were complicated by high rates of surface recession (1-2 mils/sec). It was difficult to establish equilibrium conditions due to rapidly changing geometry. SiC was selected for more refined studies since surface recession rates would be low and the sample geometry would be stable. Cylinders of KT-SiC 0.5-inch diameter by 1-inch long were used. A blackbody hole, 0.125-inch diameter by 0.6-inch deep was drilled in each sample. Three sensing devices were used to measure temperatures: (1) a micro-optical

pyrometer (0.65μ) sighted on the top surface (stagnation point), (2) a two-color Milletron pyrometer sighted at the same point, and (3) a micro-optical pyrometer (0.65μ) sighted on the base of the blackbody hole. With this arrangement, true and apparent temperature of the surface could be measured. These data would yield a reasonably good estimate of emittance. Results of several repetitive tests in static air are plotted in Figure 20.

The Milletron and blackbody hole readings are in excellent agreement from 2200° to 3000°F. These data indicate that true surface temperature is being recorded by the Milletron and that no significant temperature gradient exists through the 0.4-inch thick wall of the sample. The apparent surface temperatures when plotted against the hole temperature indicate that the emittance is between 0.65 and 0.70μ. These results are in good agreement with published data on KT-SiC.

Sightings with the Milletron were made on both the top and side wall during static and flowing (50-142 fps) tests. Results are summarized in Figure 21. Under static conditions, the side wall and blackbody hole temperatures were in good agreement. Top temperature was low compared with the side wall. This was found to be due to a crack in the sample. With flowing gas, sidewall temperature dropped 50° to 100°F. Separation of the flow due to use of a flat face specimen results in little cooling of the sides. The top, however, was cooled significantly by the impinging air. The top (stagnation) temperature dropped by 300° to 400°F below the static values. This is comparable to the effect observed with graphite specimens.

Results of these tests indicate that blackbody holes are a poor choice for use in measurement and control of test temperature in cold gas flow tests. Thus it was decided to measure and control the top (stagnation) surface temperature with the Milletron two-color pyrometer. Calibration was checked weekly to assure accurate data. The top and blackbody hole temperatures also were measured with micro-optical pyrometers and recorded for use in calculating emittance and temperature gradient data.

A major problem developed in attempts to test Hf-Ta-Mo and ZrB_2. A constant high temperature could not be maintained after a few minutes exposure to flowing air. The behavior of these materials is illustrated in Figure 22. A test with ZrB_2 was run at 3500°F in air flowing at 150 fps. After 5 minutes, a temperature of only 3200°F could be maintained at full power output. After 30 minutes, the maximum temperature of the top surface was 2800°F (at full power). At this point, the flow rate was decreased to 50 fps. Top surface temperature now increased to 3300°F at full power. However, with continued holding, temperature continued to fall and after one hour the maximum temperature at 50 fps was 2800°F. The flow rate at this point was increased to 150 fps and the temperature decreased off scale (<2000°F) on the indicating pyrometer.

The Hf-Ta-Mo alloy showed a similar behavior in a test at 3200°F in air; at 50 fps the maximum temperature dropped to 3000°F in about 20 minutes. However, temperature appeared to hold steady with continued holding at 30 minutes. It is significant to note that at 2950°F and 50 fps, a steady temperature was held with the Hf-Ta-Mo alloy for 60 minutes. Also, the temperature of coated refractory metals tested at 3400° and 3600°F was steady with time (Figure 22).

Where temperature reductions with time of holding are observed, the effect appears to be due to the formation and thickening of an insulating oxide scale. With materials and/or test temperatures where the rate of scaling is very low or negligible, steady state temperatures can be maintained. Under scaling conditions, however, surface temperature drops as the scale thickness increases. The rate of temperature drop is proportional to the rate of scaling.

A similar effect has been observed in an independent LMSC study of the oxidation of columbium. In tests of tubing heated to 2200°F by induction in air, the surface temperature was observed to decrease with time. In a controlled experiment, the metallic substrate was held constant at 2200°F by control from a thermocouple attached to the inside wall of tubing filled with argon. The temperature of the outside surface exposed to air was measured with a two-color pyrometer. Surface temperature decreased linearly with time at a rate of 1.5°F per minute. After one hour, the surface temperature was 2110°F with the substrate (0.049-inch thick wall) at 2200°F. Oxidation studies have shown that scale (Cb_2O_5) growth also is linear with time after the first five minutes of test at 2200°F. The linear surface recession rate is 0.09 mil/min. and the total surface recession rate in one hour at 2200°F is 6.6 mil. Each mil of Cb converts to approximately 2.74 mils of Cb_2O_5. Hence, the oxide scale thickness at the end of one hour is about 18 mils and the temperature drop through the scale was indicated to be 90°F.

In tests with ZrB_2, total scale thickness (ZrO_2), after calibration runs to one hour, was found to be in the range of 40 to 60 mils. The temperature drop through this scale can account for some but not all of the observed surface temperature drop of 700° to 1500°F in high velocity tests (Figure 22). It is likely that substrate temperature also is decreasing due to a reduction in coupling effectiveness as the ZrB_2 substrate is consumed. In one sample used for several calibration runs, the diameter of residual ZrB_2 was reduced to 0.25-inch (initial 0.50 inch) and coupling with the coil was very poor. Changes in the surface due to oxide scale formation also may change the relative balance of heat losses due to radiation and convection. Also, if the scale tends to laminate during growth, large thermal drops due to separations within the scale or between scale and substrate will occur.

This aspect of behavior has placed a severe restriction on CG/HW flow tests with many of the selected materials. The test procedure consists of exposing a heated sample to high-velocity air for 30

to 60 minutes. The top surface temperature is measured and is maintained at a constant value throughout the test. The measured surface recession will be compared with values obtained at the same top or front surface temperature by other test procedures (i.e., HG/CW, CG/HW). Comparable data with respect to temperature and flow can be attained in the CG/HW tests using induction-heated samples where the materials either form a volatile oxide (i.e., W, Mo, C) or have a stable surface (i.e., coated materials). Where materials form a solid oxide with a highly temperature-dependent growth rate (i.e., Hf-Ta-Mo, borides, JT-series graphites), comparable test conditions cannot be attained. For example, with Hf-Ta-Mo, the original test parameters are 2900°, 3200°, 3500° and 3800°F at flow rates of 50 and 150 fps for 30 minutes per test. From Figure 22, the maximum temperature for 30 minutes at 50 fps is 3000°F. This is at the lowest end of the desired range where the surface recession rate is about 5 mils/hr. Similarly, for ZrB_2 at 50 and 150 fps, the maximum temperature for a 30-minute test is 2800°F. Although higher temperatures can be reached initially for both materials, they cannot be maintained for more than a few minutes due to the effect of scale growth on surface temperature.

In addition to the inability to sustain high surface temperatures due to scale growth, the substrate temperature in these tests becomes an uncontrolled and undefined variable. As the surface temperature starts to decrease with oxide growth, power input must be increased to maintain a constant surface temperature. Thus, while running with constant surface temperature, the temperature at the oxide/metal interface increases continuously. What effect, if any, this has on the rate of surface recession must be established. In one test on scaling of Cb at 2200°F, the substrate temperature was increased to 2700°F to hold the oxide surface temperature constant at 2200°F. Melting occurred at the oxide/metal interface. With the Hf-Ta-Mo alloy and ZrB_2, substrate temperature in tests at constant surface temperatures of 2900° to 3000°F increased to the point where severe reaction and melting with the ZrO_2 support rod occurred. This effect also is accentuated by high flow rates. Cooling of the top surface results in overheating of the bottom.

A large temperature gradient was found to exist in all samples during flow tests. This behavior, with respect to graphite and SiC, has been discussed. A similar behavior was found for the JT-graphites and for the Hf-Ta alloy. In testing JT-0992 graphite at 3600°F the oxide layer which formed on the top surface separated and mushroomed up. This caused the top to appear cool. On raising the power input to bring the top surface temperature up, the bottom of the sample overheated and fused with the ZrO_2 support rod. Temperature measurement and control with this series of graphites will be particularly difficult. Oxide scale separation and blister formation also occurred on the side wall of some samples of JT-0992 at 3600°F. A similar problem was encountered with tests of Hf-19Ta-2Mo in air at 50 fps. On trying to hold the top surface temperature at 2700°F (brightness) the side wall temperature was indicated to be 3000°F (brightness). This corresponds to true temperatures of

2900°F and 3280°F, respectively. On continued heating with the top at 3100°F, the sample reacted with the ZrO_2 support and localized fusion occurred. The lower half of the specimen melted, terminating the test.

Problems of reaction between specimens and the ZrO_2 stinger also were encountered in tests of coated tantalum - 10% tungsten and tungsten cylinders. With both materials coating failure was initiated by eutectic melting of oxides (Al_2O_3, SiO_2, Ta_2O_5 and WO_2) with ZrO_2 in tests at 3400° to 3600°F. The use of a helium purge through the ZrO_2 stinger to reduce or prevent oxidation at points of contact was tried without success. The problem was solved by holding the samples on a water-cooled copper stinger. This prevented contact failures and permitted evaluation of coating performance on flow-exposed top surfaces. The use of a water-cooled stinger also solved the problem of overheating the bottom of samples in high-velocity tests. The temperature gradient effectively is reversed to one of hot at the top to cold at bottom. Tests were run successfully with a 3/8-inch long by 1/2-inch diameter W/WSi_2 sample heated to 3680°F on the top surface with the bottom surface in contact with water-cooled copper. No reaction occurred at contact points. The bottom of Hf-Ta-Mo samples with the top surface heated to 3000°F was only lightly discolored at the point of contact with the cooled stinger. The additional heat loss through the stinger, however, further reduces the attainable temperatures for difficult-to-couple-with materials. The cooled support will be used only for those materials where contact reactions cause premature failure or shutdown of the test.

4. Measurement of Emittance

The design and operation of the CG/HW test apparatus afforded an excellent opportunity to measure emittance at high temperature in an oxidizing environment. Extensive tests with many materials show that emittance changes both with temperature and with alteration of the surface (oxide film or scale formation). Measurements were made to determine the approximate emittance correction for the oxidized surface of the Hf-19Ta-2Mo alloy. The brightness (micro-optical 0.65μ) and true (Milletron-two-color) temperatures were read simultaneously on the top surface of a sample heated in air. The results are shown in Figure 23. The calculated normal spectral emittance (0.65μ) was found to decrease with increasing temperature from a value of 0.6 at 2400°F to 0.42 at 3400°F. This effect is not one of changing surface conditions with time during the calibration. The low temperature readings were taken first and the high temperature readings last. At the end of the run, the low temperature reading was checked again and the result was in perfect agreement with the initial calibration point. The LMSC Milletron was checked against the ManLabs' Milletron by sighting both units on the top surface of a heated sample. The LMSC unit consistently indicated higher temperatures with a +10°F differential at 3300°F, and a +18°F differential at 3550°F. This is less than 1% error in reading and is considered excellent agreement. The calibration check was made on the surface of a Hf-19Ta-2Mo sample heated in static air.

The foregoing example serves to illustrate that useful data can be obtained by this approach. It is recognized that the normal spectral emittance obtained in this manner is not a precise or highly accurate determination. However, the data are valid approximations that can be extremely useful in evaluating the behavior and performance capabilities of refractory materials. Since virtually no data on emittance of these materials are available, the data obtained in this study provides a needed starting point.

C. Temperature Gradients through Oxide Scale

Two methods were developed for measuring the temperature gradients through oxide scales on the surface of induction heated samples. In the first method, the metal/oxide interface temperature was measured by a Pt/Pt-Rh thermocouple while the surface temperature was measured with an optical pyrometer. This method is limited to temperatures of about 3000°F and was used to study gradients in a Cb_2O_5 scale formed on Cb-1Zr alloy. A thermocouple well was drilled down the center of a 0.3 x 0.3 x 0.75 inch sample to within 0.060 inch of the surface. The sample was supported vertically within an induction coil using the thermocouple insulating sleeve (alumina) as a stinger. The thermocouple bead was bare and made direct contact with the metal at the base of the drilled hole. Helium gas was passed up the alumina support rod to shield the internal surfaces and contact area from oxidation. Surface temperature was measured with a micro-optical pyrometer using a previously established normal spectral emittance of 0.59 to convert from brightness to true temperature. Samples were heated for 30 to 60 minutes holding either the surface (T_S) or metal (T_M) temperature constant and measuring the corresponding temperature at the uncontrolled site (surface or metal) at 5-minute intervals. The results are shown in Figure 24.

Initially, the indicated temperatures for the top surface and the substrate were within +10°F of each other. With the metal temperature held constant at 2200°F, surface temperature decreased gradually with time of holding. After 1 hour, the surface was at 2100°F while the substrate was still at 2200°F, the metal temperature increased with time of holding. After 50 minutes, the metal substrate was 150°-200°F hotter than the surface. The time rate of change in temperature for both cases is shown in Figure 24.

In the second method used to study this effect, the substrate or interface temperature was measured with a micro-optical pyrometer while the true surface temperature was measured with a two-color pyrometer. This approach was used for tests above 3000°F where contact thermocouples could not be used. A 0.25-inch diameter hole was core drilled along the center line of a 0.5-inch diameter by 1-inch long cylindrical sample to within about 150 mils of the top surface. The specimens were supported on alumina, zirconia, or water-cooled copper tubular stingers having a 0.125-inch inside

diameter. Helium was passed slowly up the tube to prevent oxidation of the substrate and to clear out smoke or vapors. A calibrated front surface mirror was positioned to sight up the tube for optical measurement of substrate temperature. Brightness readings were converted to true temperature using previously established emittance corrections.

This method was used to study the temperature gradients through ZrO_2 scales formed on ZrB_2 samples heated to 3400°F in air flowing at 50 fps. The behavior was identical to that observed in tests of the Cb-1Zr alloy. As shown in Figure 25, the surface temperature decreased with time as the substrate was held constant at 3400°F. After 1 hour, the surface was 220°F cooler than the induction-heated core. The gradient here is more than double that observed in tests with Cb-1Zr alloy at 2200°F. Similarly, as shown in Figure 25, the metal (boride) temperature increased rapidly in tests where the surface was held constant at 3400°F. After 20 minutes, the substrate was 250°F hotter than the surface. This is about 3 times the gradient observed with Cb-1Zr at 2200°F. Figures 26-29 show post exposure photographs of samples ZrB_2(A-3)-13(L45-1) and ZrB_2(A-3)-18(L46-1) after CG/HW exposures at 50 ft/sec air flow. In both cases, the oxide thickness is about 15 mils and the boride wall thickness is 100 mils.

Two tests with $HfB_{2.1}$(A-2) reveal a behavior like that observed with ZrB_2. At low temperatures (3400°F) where the recession rate is low, steady state surface temperatures could be maintained. At higher temperatures where the recession rate is rapid, scale growth results in a continuous temperature drop. This behavior is summarized below:

	Surface Temperature (°F)	
	Slow Recession	Fast Recession
Time (min)	Run 38-1 $HfB_{2.1}$(A-2)-13	Run 39-2 $HfB_{2.1}$(A-2)-15
0	3400	3600
5	3400	----
10	3400	3520
15	3400	3400
20	3400	3420
25	3400	3420
30	3400	3350
40	3400	3300
50	3400	3250
60	3400	3190

In the fast recession rate tests, full power input was maintained and the indicated temperature is the maximum attainable at a flow rate of 50 fps. Assuming the substrate to be at 3600°F or even higher, a

temperature gradient of over 400°F through the oxide scale is indicated. Figures 30-33 show photomicrographs of $HfB_{2.1}$(A-2)-13(L38-1) and $HfB_{2.1}$(A-2)-15(L39-2) after exposure. The latter sample cracked after cooling. Metallographic examination showed that the $HfB_{2.1}$(A-2) material contained porous bands. Sample $HfB_{2.1}$(A-2)-15 also exhibited several shallow cracks which might have led to failure.

A fourth series of tests to study temperature gradients was conducted with 0.5 inch diameter by 1 inch long cylinders of Hf-20Ta-2Mo (I-23) alloy. Five samples were drilled to form closed-end cylinders with a minimum wall thickness at the top of 0.12 to 0.15 inch. In the first test (44-1), the sample was supported on a 0.25-inch OD x 0.10 inch ID ZrO_2 tube and was purged internally with helium to prevent oxidation. The top surface temperature was measured and held constant at 3400°F using the Milletron two-color pyrometer. A micro-optical pyrometer (0.65μ) was sighted up the tube to measure substrate temperature. The alignment was poor, however, and no useful readings could be obtained. The test was terminated at 30 minutes when full power was required to maintain the surface at 3350°F in air flowing at 1 to 10 fps. The sample had a light grey adherent scale on the top surface and a thick white scale on the side walls. It cracked on cooling and broke into two pieces. Figures 34 and 35 show post exposure photographs of this sample.

In a second test (44-2), the sample was supported on an Al_2O_3 tube having a 0.22-inch ID hole. This permitted better sighting with the micro-optical pyrometer and good measurements of substrate temperature were obtained. An emittance value of 0.55 was assumed for calculation of substrate temperature. Figures 36 and 37 show photographs of this sample after testing. The following three tests were conducted maintaining the metallic substrate at constant temperature. In tests (44-1 and 44-2) the samples reacted and fused with the ZrO_2 and Al_2O_3 support tubes. It is necessary to support the samples on nonreactive materials and previous experience has shown that water-cooled copper is very good for this purpose. A new support stinger was designed and built from hand drawing 0.25 inch OD copper tube. The outside surface and specimen support were water cooled. The inside was open and was connected to a gas purge system and a front surface mirror for temperature measurement. With this device, internal temperature could be measured while using a helium purge to prevent oxidation of the sample from the inside. The outside diameter of the completed stinger was 0.5 inch. This matches the specimen diameter and minimizes disturbance of the air stream. All subsequent tests were conducted using this support.

In run 44-2, the surface temperature initially was about 45°F higher than the substrate temperature. Normally, the surface should be cooler because of air flow effects. This may be due to an error in the assumed value of emittance. The internal surface was purged with helium and did not develop an oxide scale. If the actual value of emittance was less than 0.55, the substrate temperature would be higher than the calculated value of 3355°F. It also is possible that at the low flow rate used, very little cooling of the surface occurs. The

surface temperature held constant for about 20 minutes and then began to decrease slowly with time. At the end of 60 minutes, the surface temperature was 3220°F with the substrate still at 3350°F. This behavior is very similar to that found for Cb-1Zr and the borides.

The last three runs (76-1, 77-1 and 77-2) were conducted in air flowing at 50 fps using substrate temperature control. In each case, the initial surface temperature was 320° to 400°F lower than the substrate temperature with wall thickness of 0.11 to 0.15 inch, illustrating the significant effect of air flow on cooling of the surface. Metal temperature below the oxide scale is assumed to be close to that reported for the substrate measurement. Again, an emittance value of 0.55 was assumed to calculate true temperature. Actual values may be somewhat higher due to the use of an internal helium purge to minimize oxidation. In all tests, top surface temperature decreased with time. After 60 minutes, the surface temperature was 400° to 500°F lower than the substrate temperature. Figures 38-41 show post exposure photomicrographs of these samples.

It is obvious from these tests that significant temperature gradients can be developed across thin oxide scales formed on the surface of metals or intermetallic compounds during oxidation (scale thicknesses ranged between 0.010 and 0.060 inch). The gradient results from the formation of an insulating oxide scale on the surface. With induction heating, the metallic substrate is heated directly by coupling with the electromagnetic field. The nonconducting oxide scale, however, does not couple with the field and is heated indirectly by conduction from the heated substrate. The surface is cooled by radiation and convection. This leads to an inverse gradient in which the temperature at the metal/oxide interface is higher than that at the oxide/air interface. As the oxide thickens with time, the resistance to heat transfer is increased. If the substrate temperature is held constant, surface temperature will decrease. If the surface temperature is held constant, the substrate temperature must be increased to overcome the added resistance to heat flow.

The importance of this aspect of materials behavior depends upon the rate-controlling factor in the oxidation process. Since the surface temperature is measured and controlled in most tests of materials, oxidation data will be accurate only if surface temperature controls the reaction rate. If the substrate or interface temperature is rate controlling, however, the measured rate of oxidation will be too high or too low, depending on the method of heating used in conducting the tests. If the substrate is heated by induction or direct resistance, it will be hotter than the surface. If the surface is heated by radiation, the substrate may be cooler or at the same temperature, depending on heat losses to supporting devices or structures. In most gas torch or plasma tests, the substrate will be cooler than the surface. Only in furnace tests where the sample is brought to a uniform temperature throughout, will the surface and substrate be at the same temperature. This aspect of materials behavior is discussed in detail in Part III, Volume II of this series of reports.

REFERENCES

1. Kaufman, L. and Clougherty, E.V., "Investigation of Boride Compounds for Very High Temperature Applications," RTD-TDR-63-4096 Part III, March 1966

2. Kaufman, L., Clougherty, E.V., and Berkowitz-Mattuck, J.B., Trans. Met. Soc. A.I.M.E. (1967) 239 458

3. Berkowitz-Mattuck, J.B., Kaufman, L., Clougherty, E.V., and Hopper, R., Trans. Met. Soc. A.I.M.E. (1967) 239 750

4. Clougherty, E.V., Pober, R.L., and Kaufman, L., Trans. Met. Soc. A.I.M.E. (1968) 242 1077

5. Berkowitz-Mattuck, J.B., J. Electrochem. Soc. (1964) 111 908

6. Berkowitz-Mattuck, J.B., J. Electrochem. Soc. (1966) 113 908

7. Berkowitz-Mattuck, J.B., J. Electrochem. Soc. (1967) 114

8. Littman, C., and Berkowitz-Mattuck, J.B., Rev. Sci. Inst. (1961) 32 1154

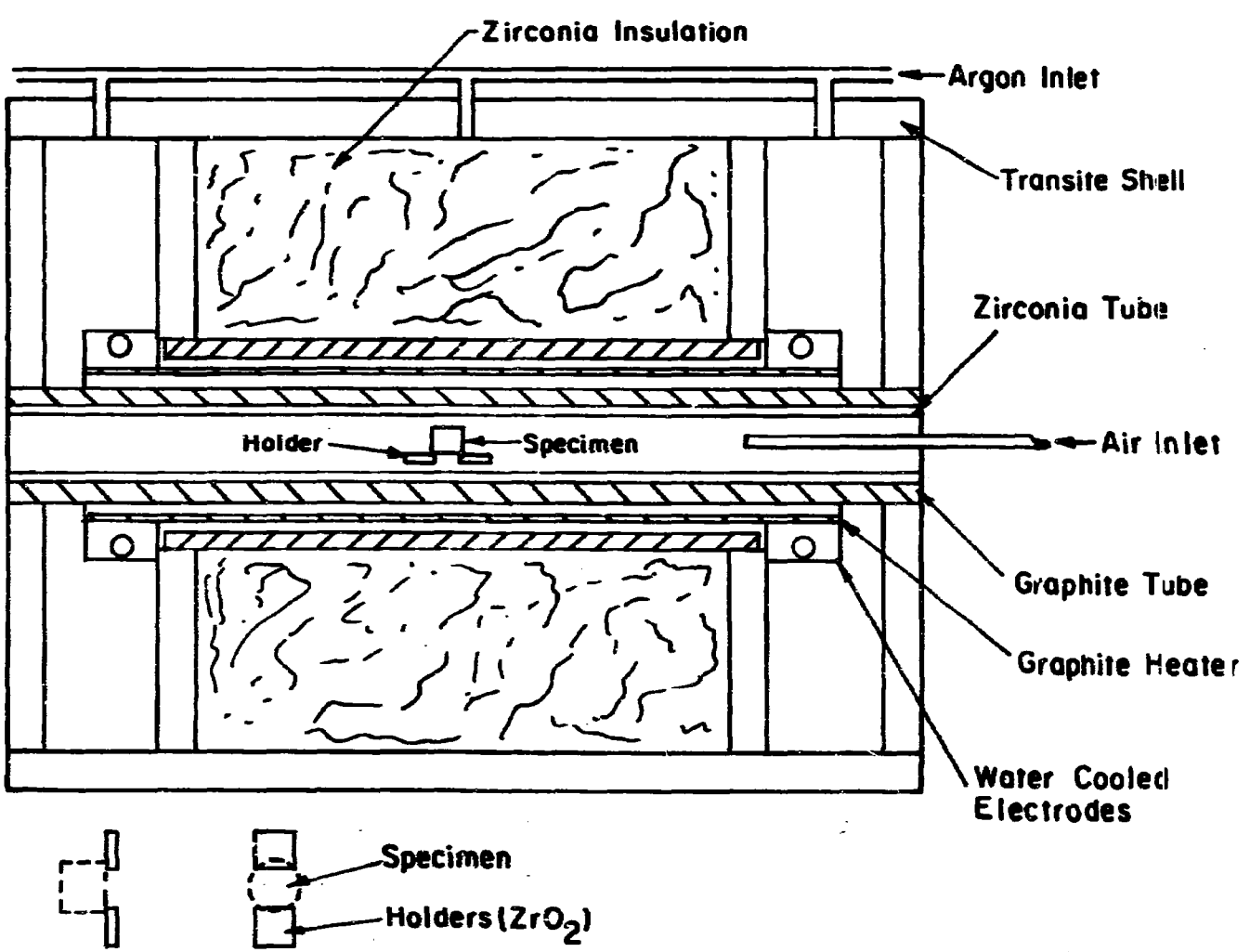

Figure 1. Schematic Diagram of Air Oxidation Furnace.

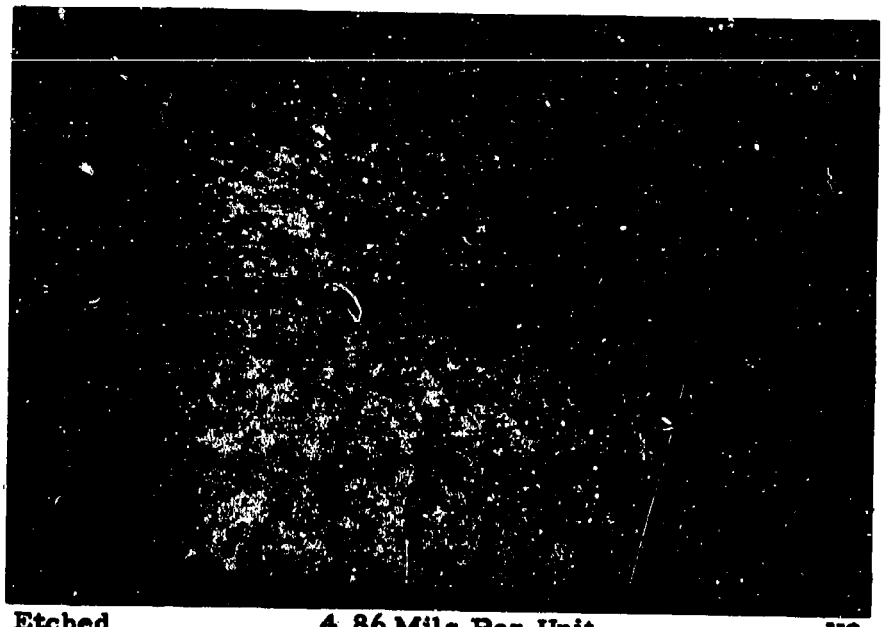

Plate No.
1-1930

Etched 4.86 Mils Per Unit -X8

Figure 2. $HfB_{2.1}$ (A-2), OX-268 (60 Min. at 3209°F), Longitudinal Section. Conversion Depth 16 Mils.

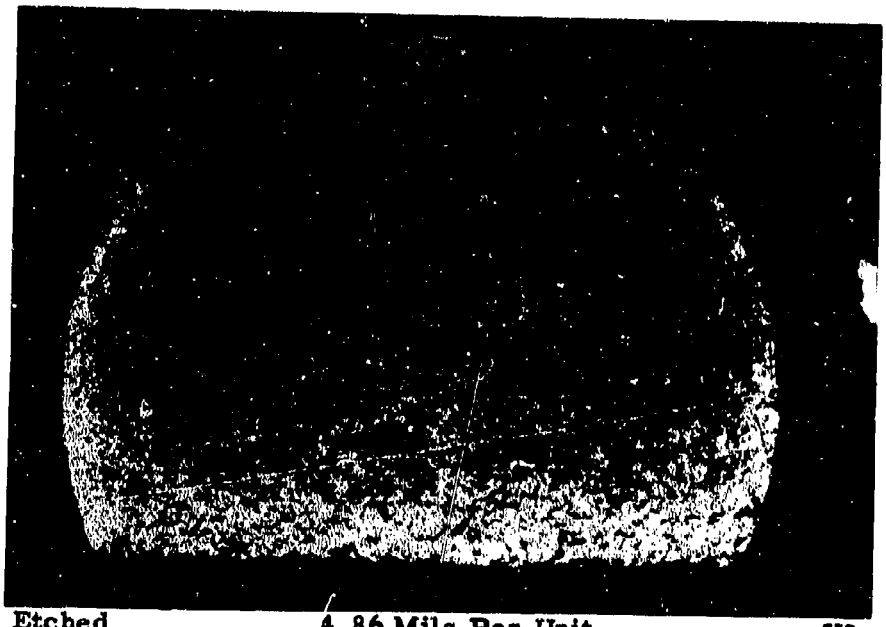

Plate No.
1-1933

Etched 4.86 Mils Per Unit -X8

Figure 3. $HfB_{2.1}$ (A-2), OX-268 (60 Min. at 3209°F), Transverse Section. Conversion Depth 16 Mils.

Plate No.
1-1931

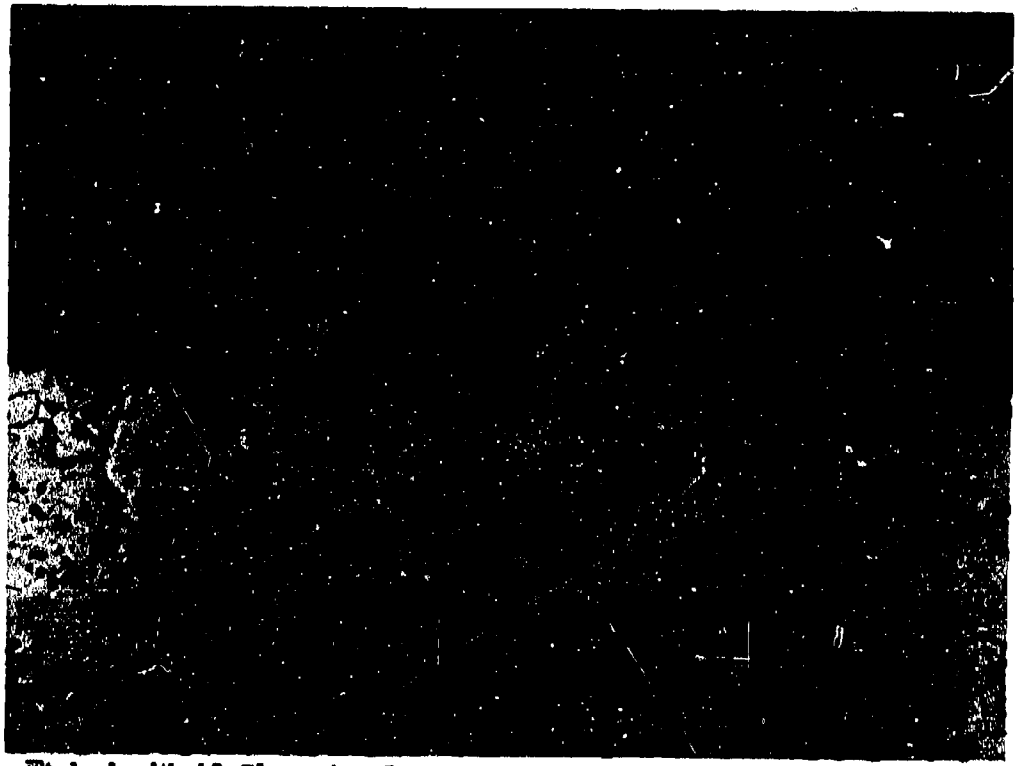

Etched with 10 Glycerine 5HNO_3 3HF X250

Figure 4. $HfB_{2.1}$ (A-2), OX-268 (60 Min. at 3209°F), Interface of Longitudinal Section.

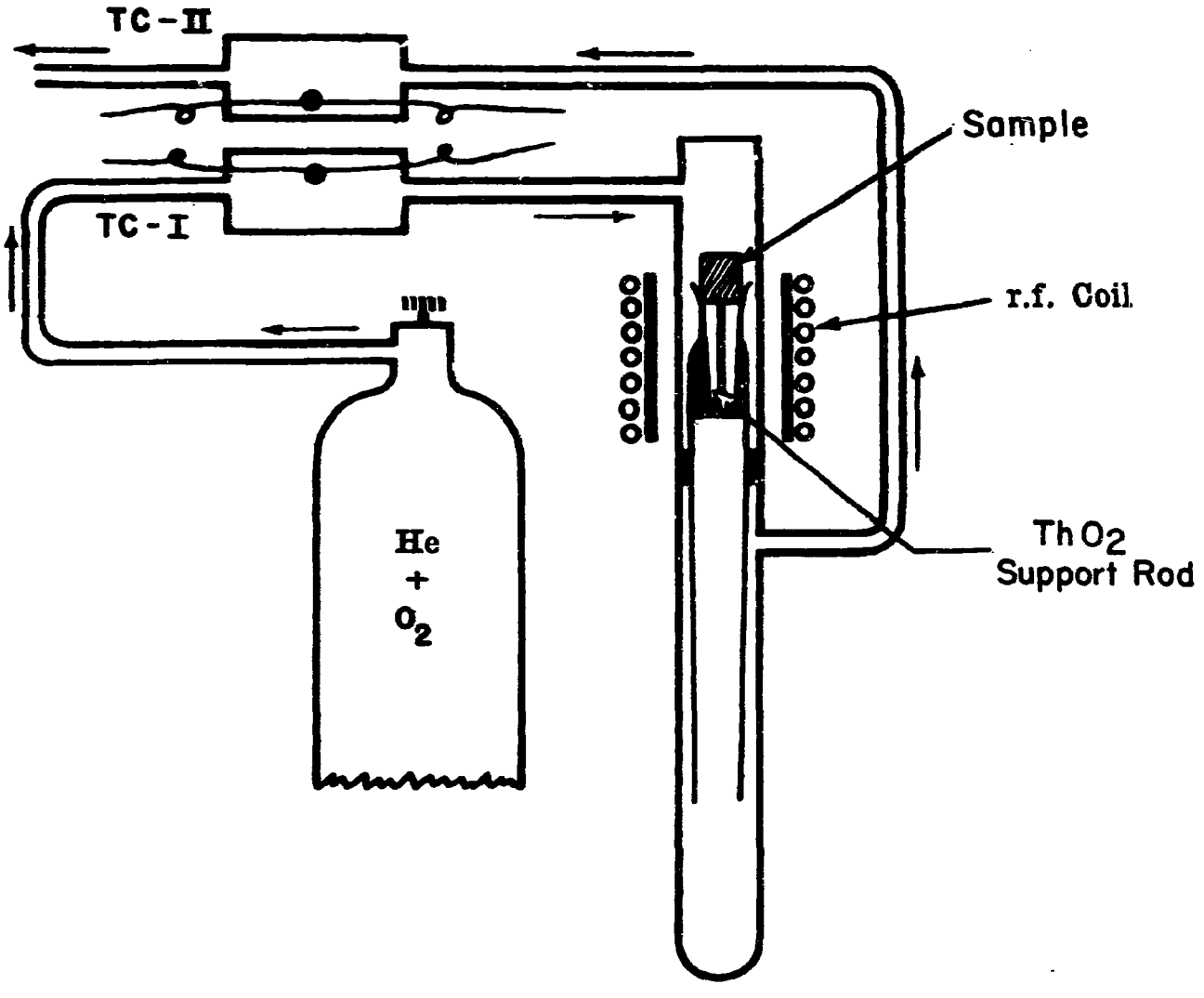

Figure 5. Schematic Drawing of Arrangement for Monitoring Rates of Oxygen Depletion and Carbon Monoxide and Carbon Dioxide Formation.

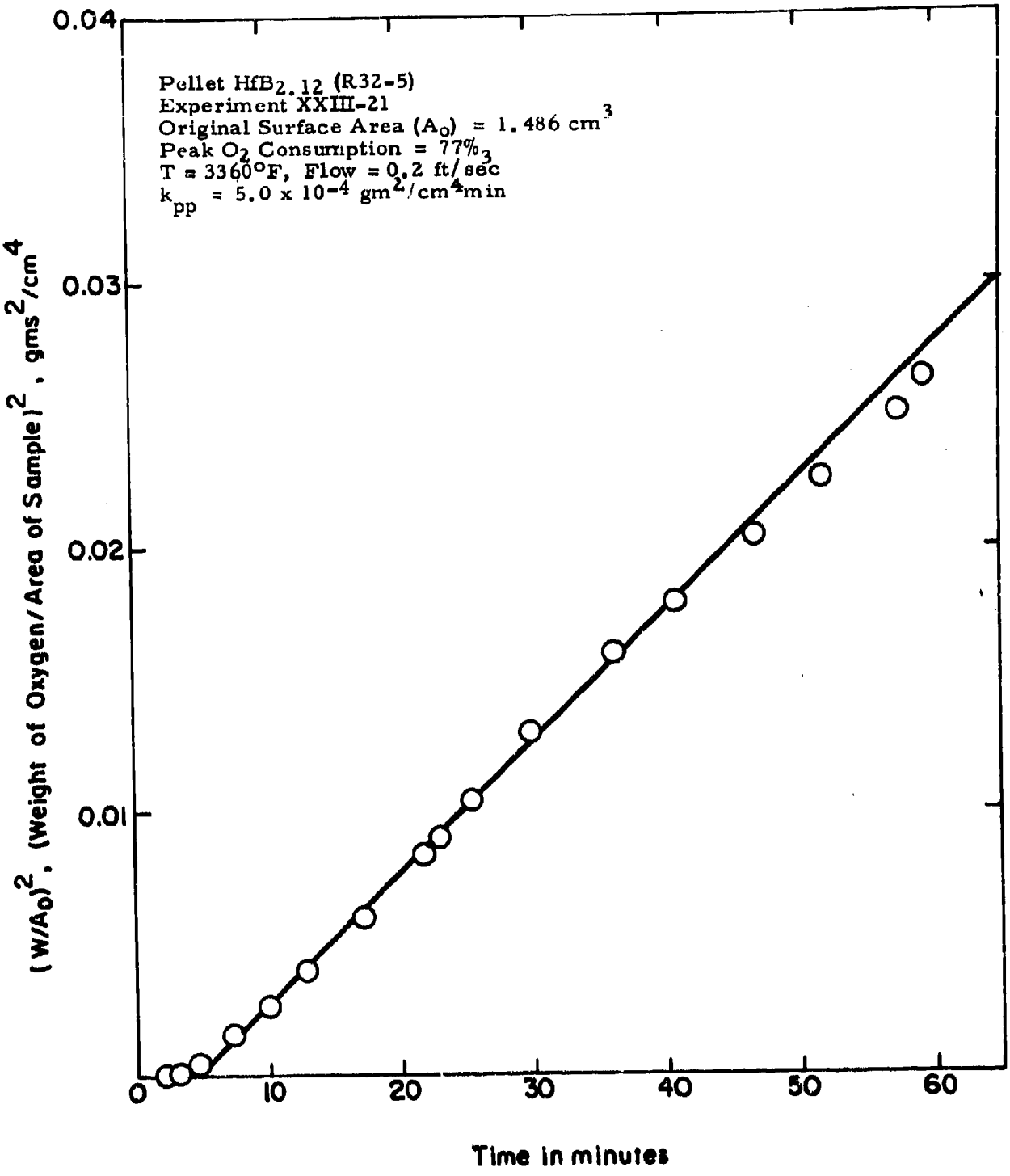

Figure 6. Weight of Oxygen Consumed as a Function of Time Determined in Thermal Conductivity (Oxygen Pickup) Experiment XXIII-21.

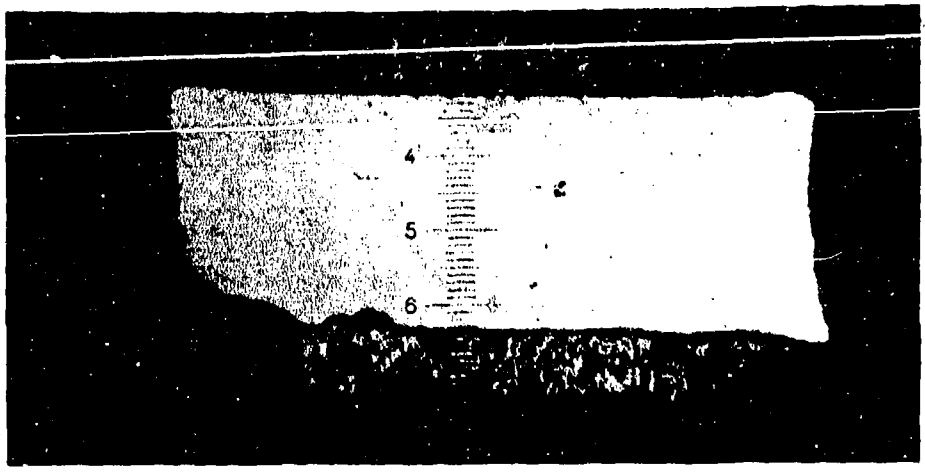

Plate No.
1518

Unetched 1.97 mils/unit

Figure 7. Pellet XXIII-21 (R32-5) $HfB_{2.12}$, after Oxidation at 3360°F for One Hour, Showing Longitudinal Section. Initial Height 93 mils, Final Height 61.6 mils, Depth of Conversion 15.7 mils. Calculated Depth from Thermal Conductivity Measurement 15.8 mils.

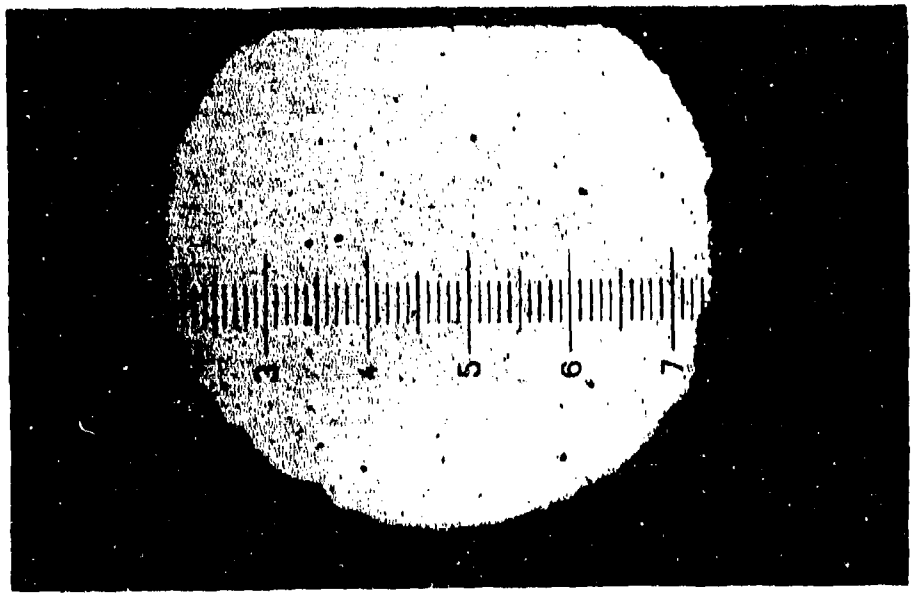

Plate No.
1699

Unetched 4.86 mils/unit

Figure 8. Pellet XXIII-21 (R32-5) $HfB_{2.12}$, after Oxidation at 3360°F for One Hour, Showing Transverse Section. Initial Diameter 301 Mils, Final Diameter 270 Mils, Depth of Conversion 15.5 Mils. Calculated Depth from Thermal Conductivity Measurement 15.8 mils.

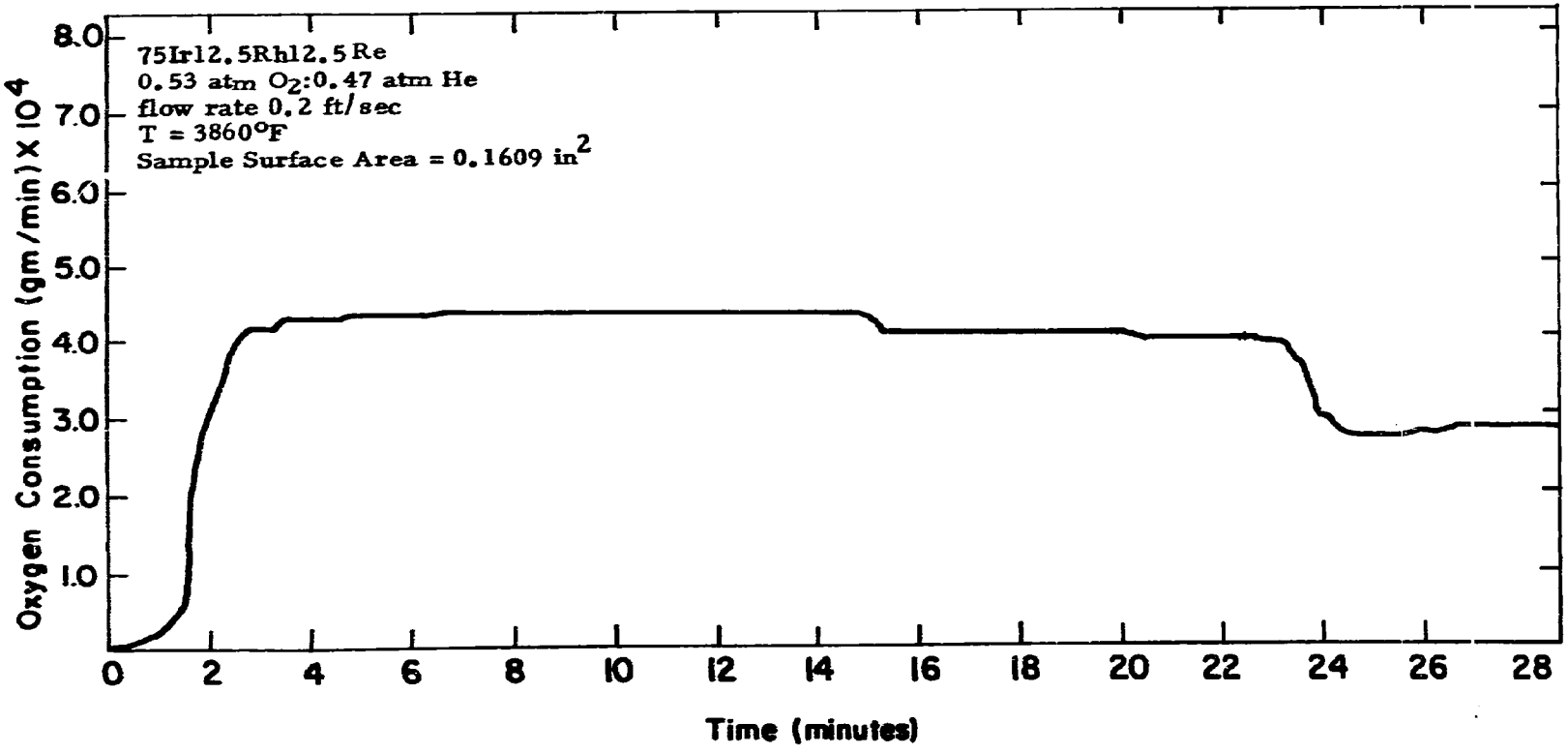

Figure 9. Oxygen Consumption Vs. Time for 75Ir12.5Rh12.5Re at 3860°F.

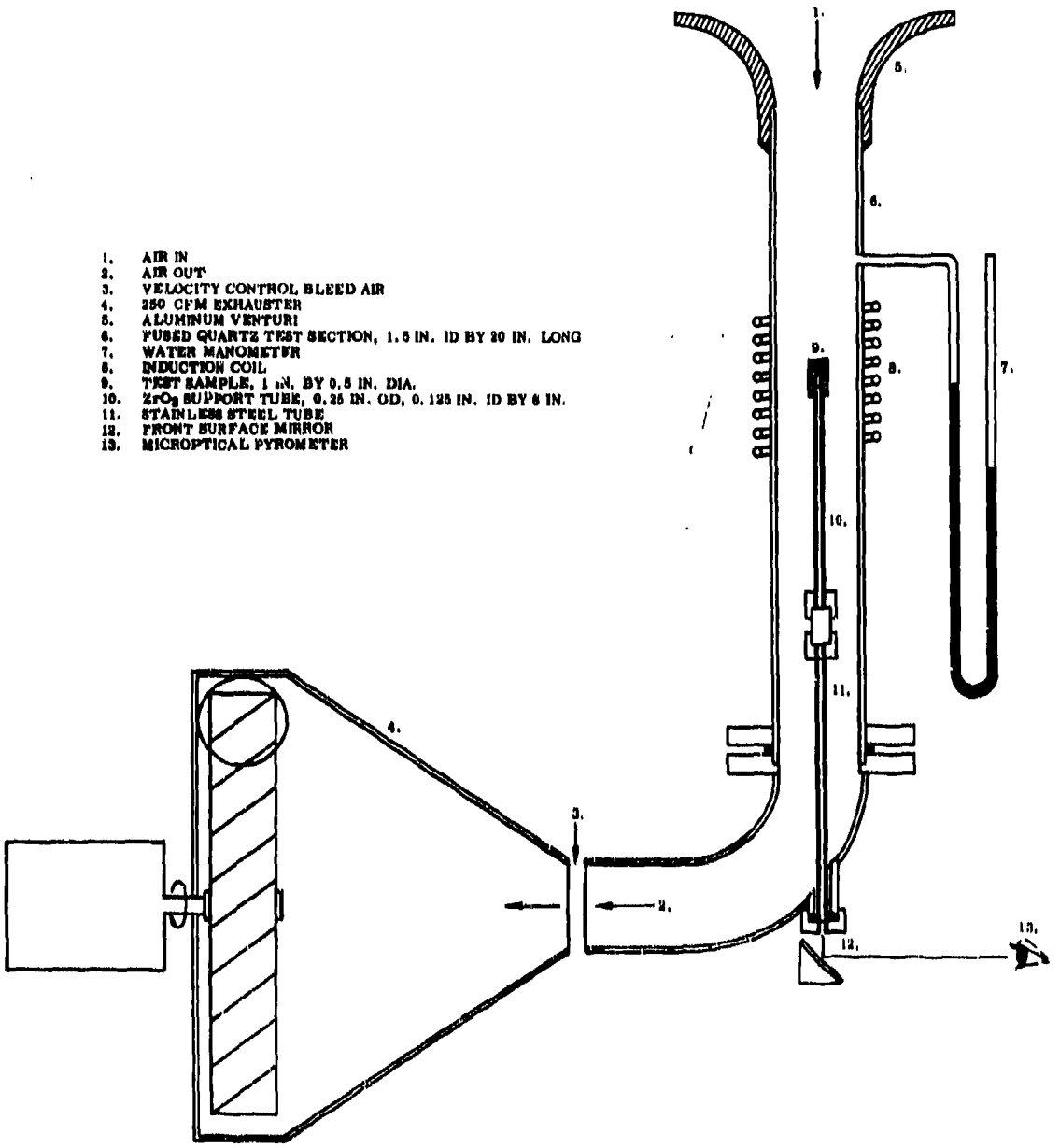

Figure 10. Schematic of Oxidation Test Unit (4000°F, 300 ft/sec).

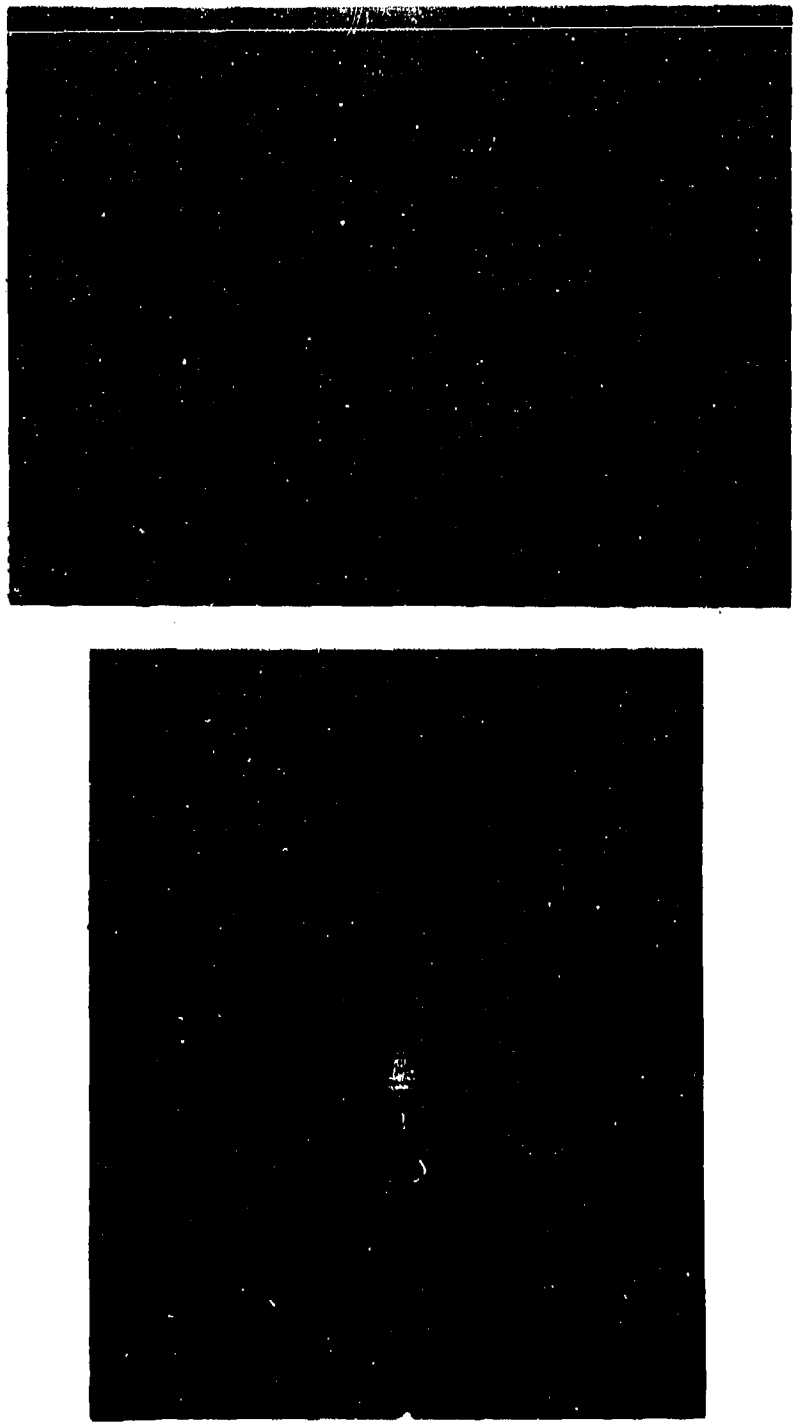

Figure 11. Oxidation Test Apparatus (4000°F, 300 ft/sec)

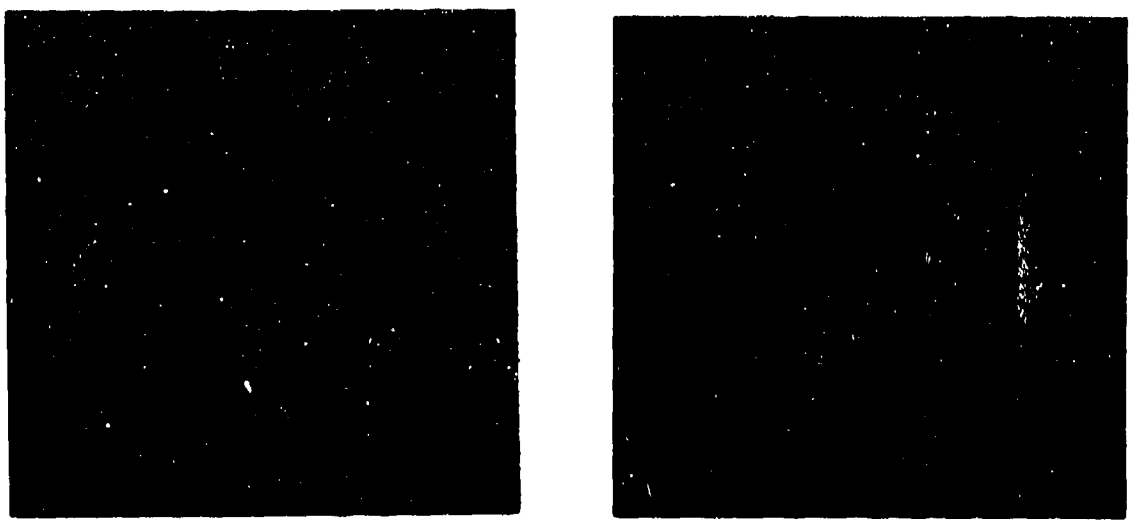

No Flow 160 ft/sec

Blunt End

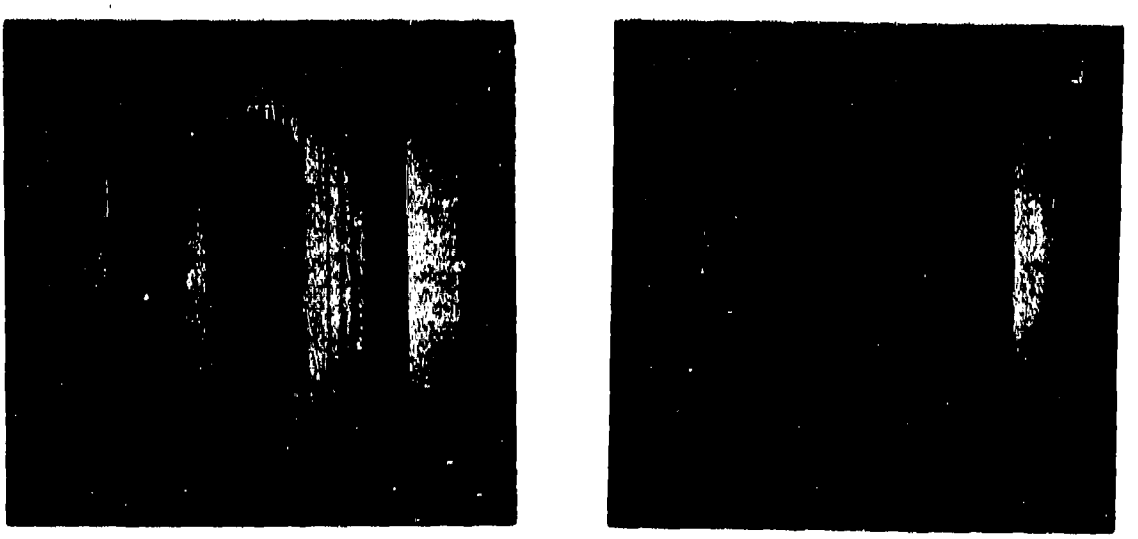

No Flow 160 ft/sec

Hemispherical End

Figure 12. Effect of Model Configuration on Flow Pattern.

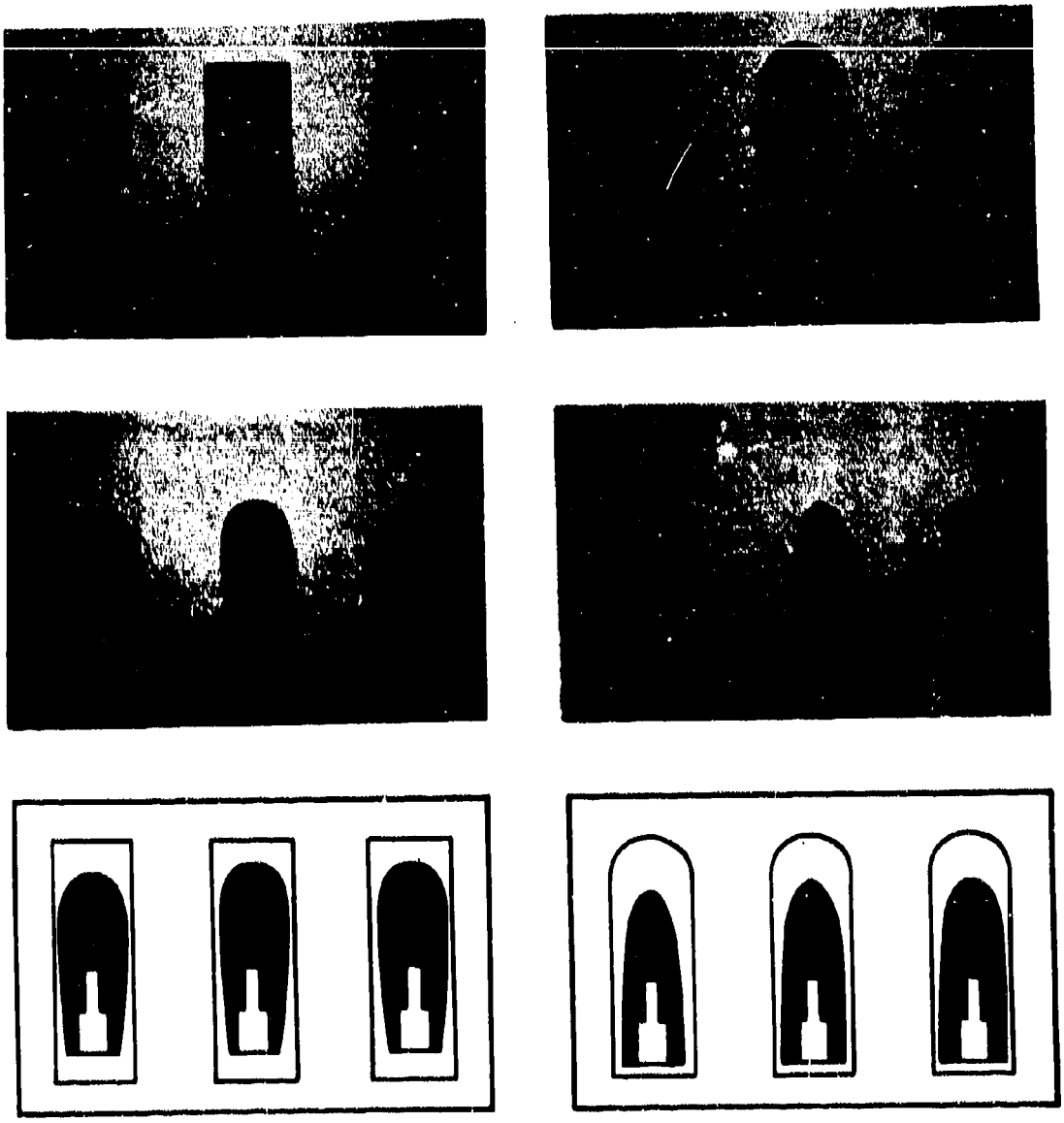

Surface Recession in Mils

270	205	210	Nose	420	360	210
140	140	140	Tail	40	40	40
47	40	37	Radius	74	64	55

Figure 13. Effect of Model Configuration on Surface Recession of Graphite (3400°F, 160 ft/sec, 2 min).

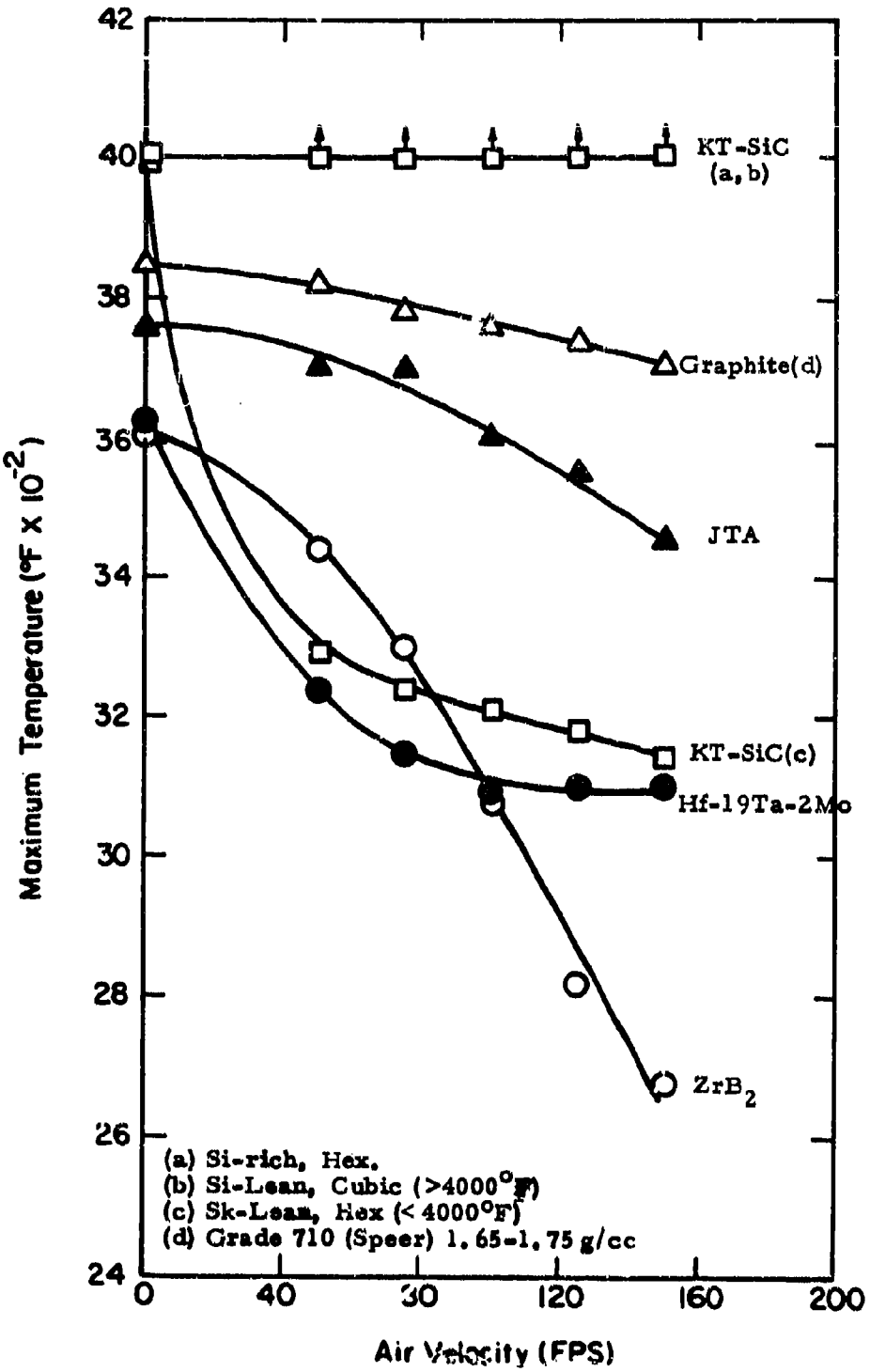

Figure 14. Test Capabilities with Lepel 475 kc - 23 kva Power Supply.

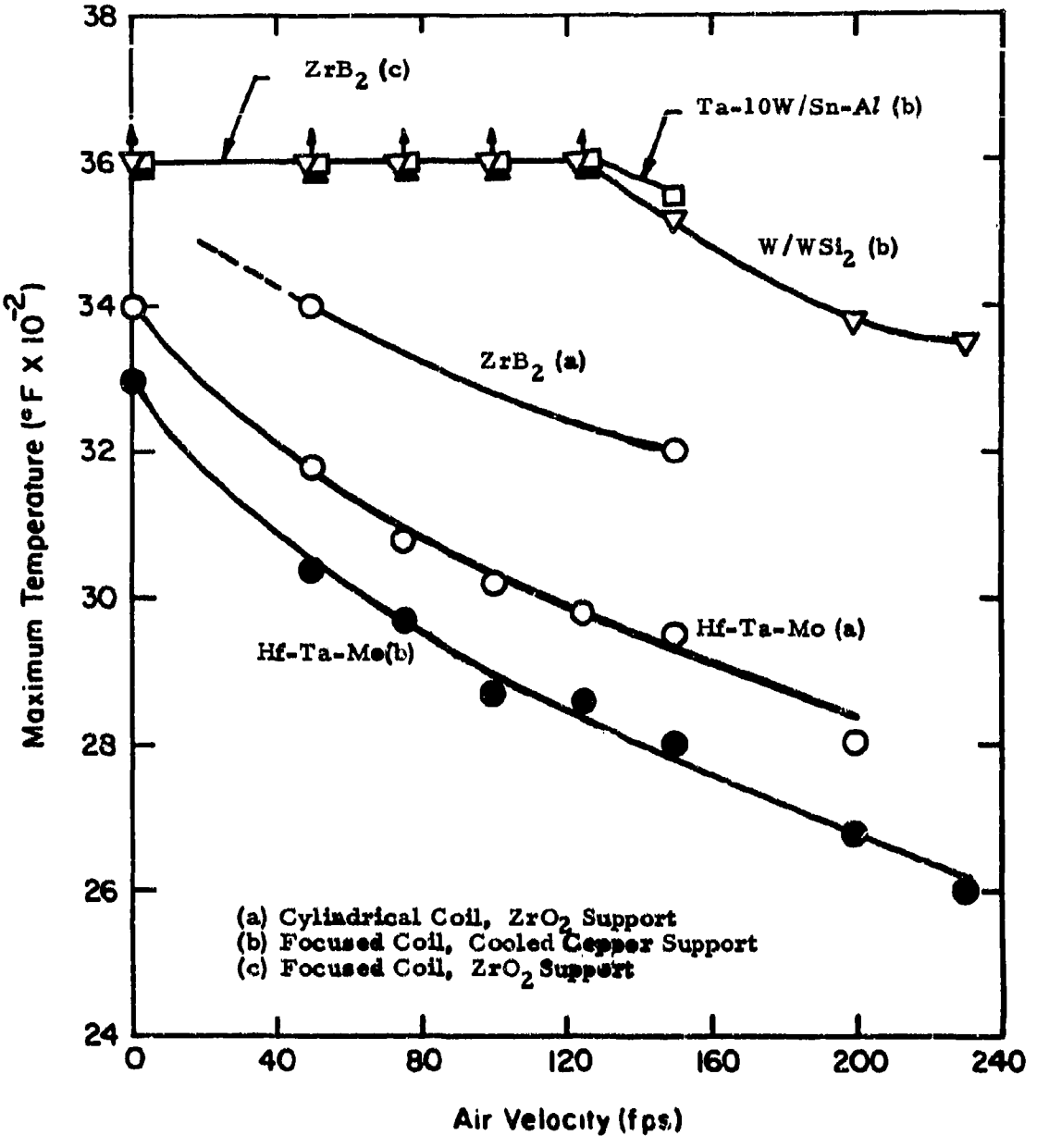

Figure 15. Test Capabilities with Tocco 30-kW, 10 kc Power Supply.

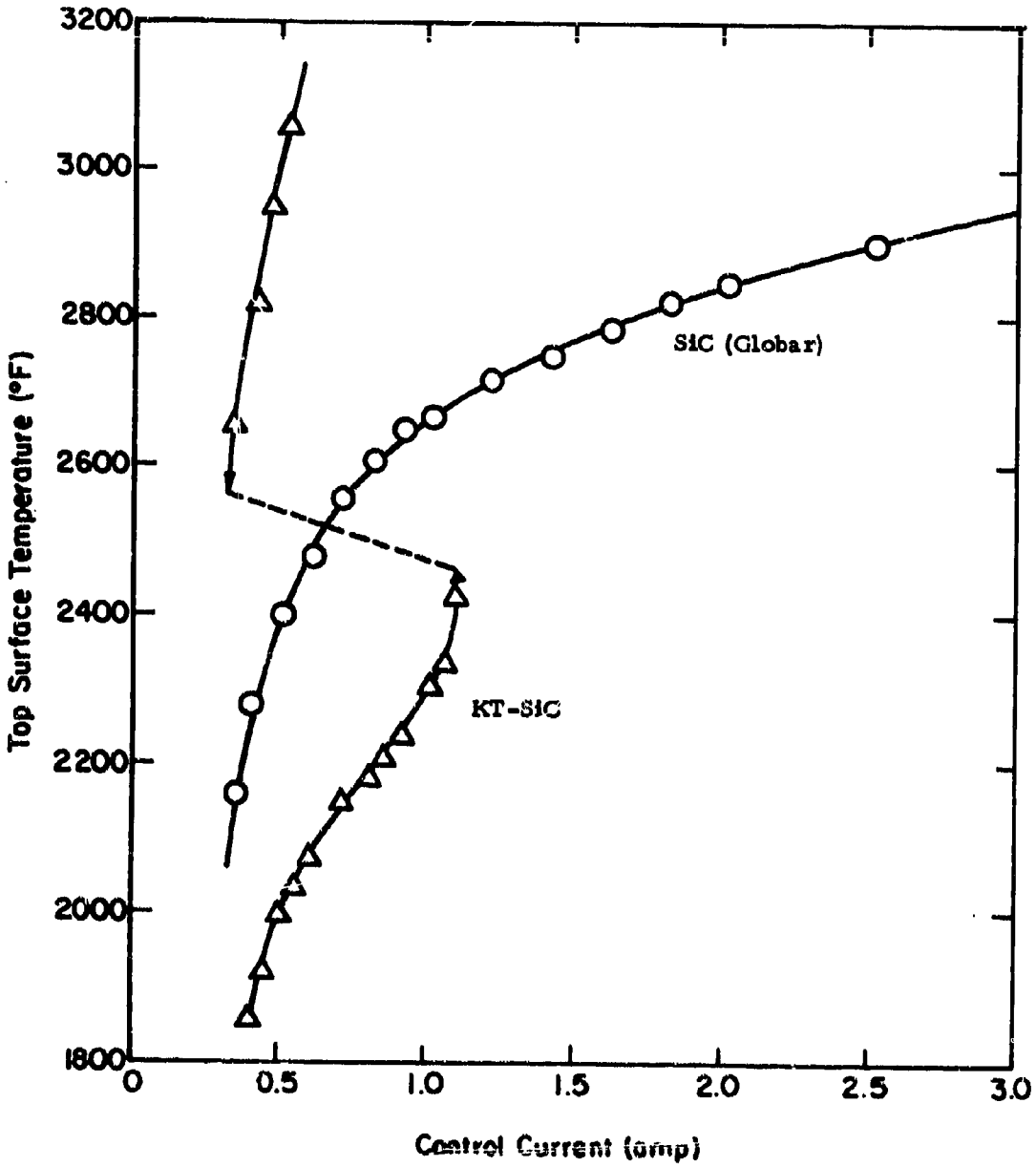

Figure 16. 2550°F Coupling Transition on Induction Heating KT-SiC.

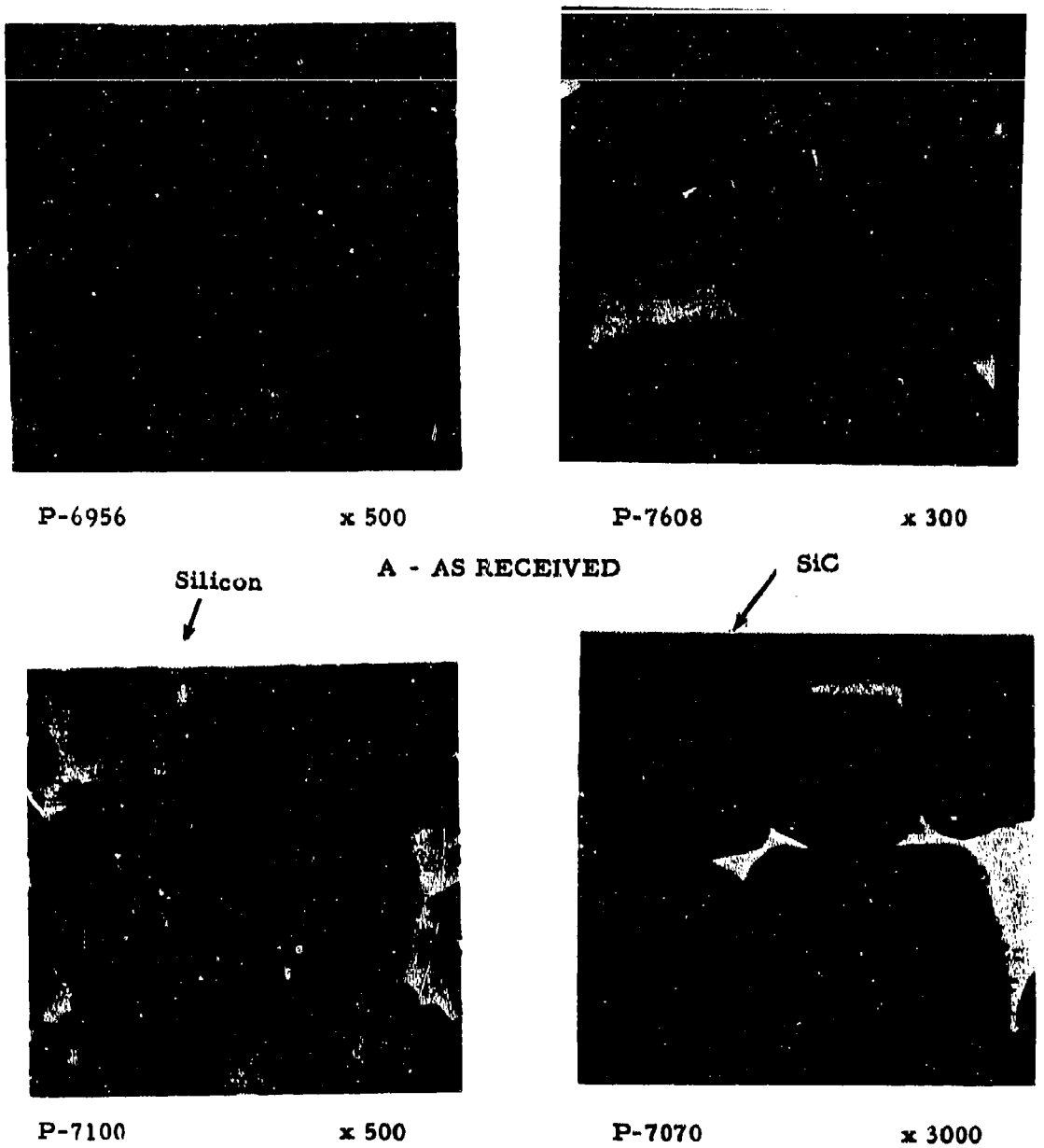

Figure 17. Structural Changes in KT-SiC on Heating Above 2550°F.

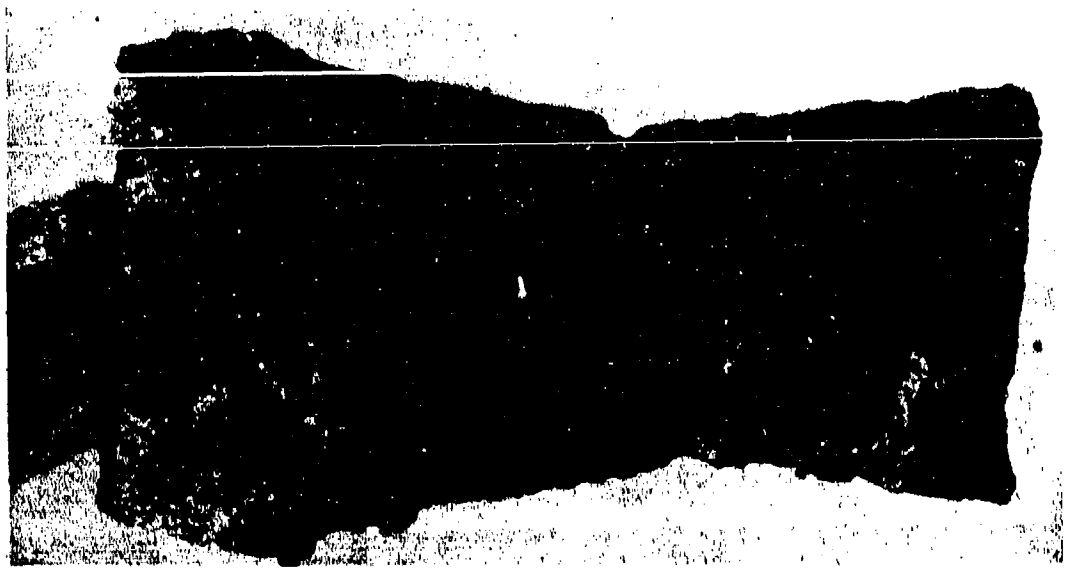

P-7255 x 5.5

A - GENERAL APPEARANCE

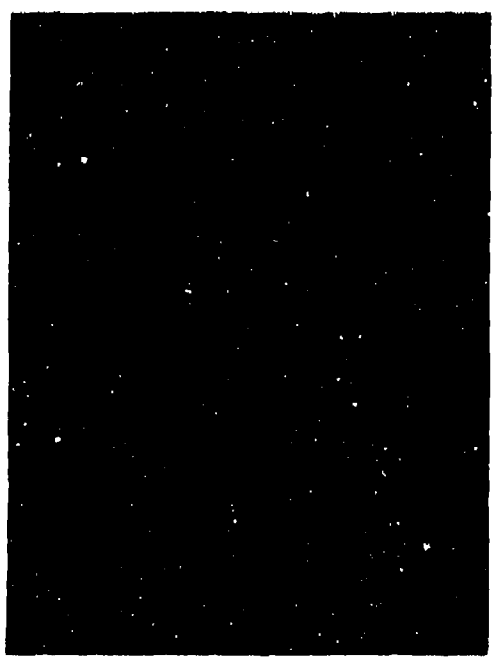

P-7606 x500

TOP

P-7608 x 500

BOTTOM

$ZrSi_2$

B - MICROSTRUCTURE

Figure 18. KT-SiC Heated to 4700°F in Air Flowing at 150 fps.

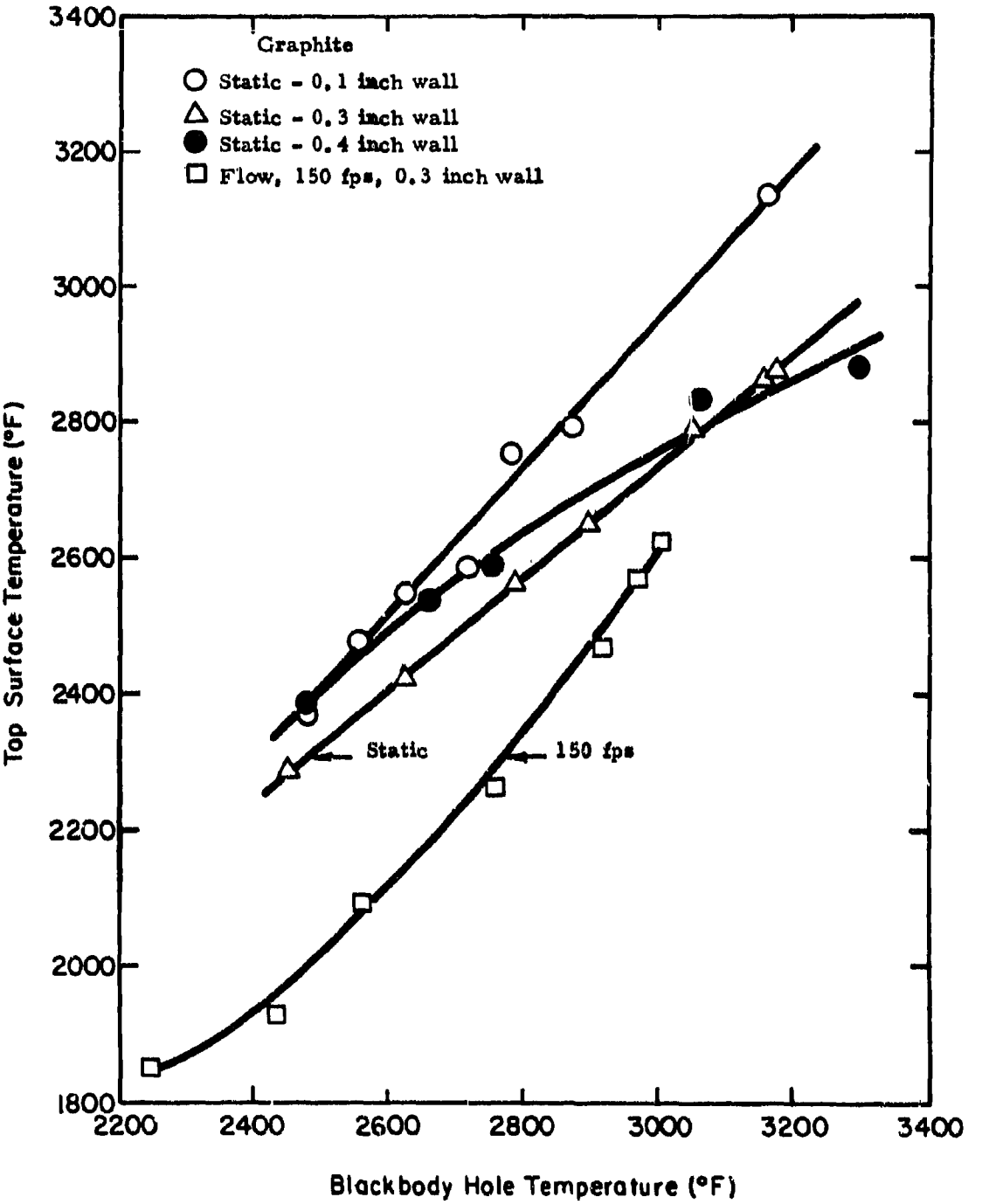

Figure 19. Temperature Relationship in Graphite Test Cylinders.

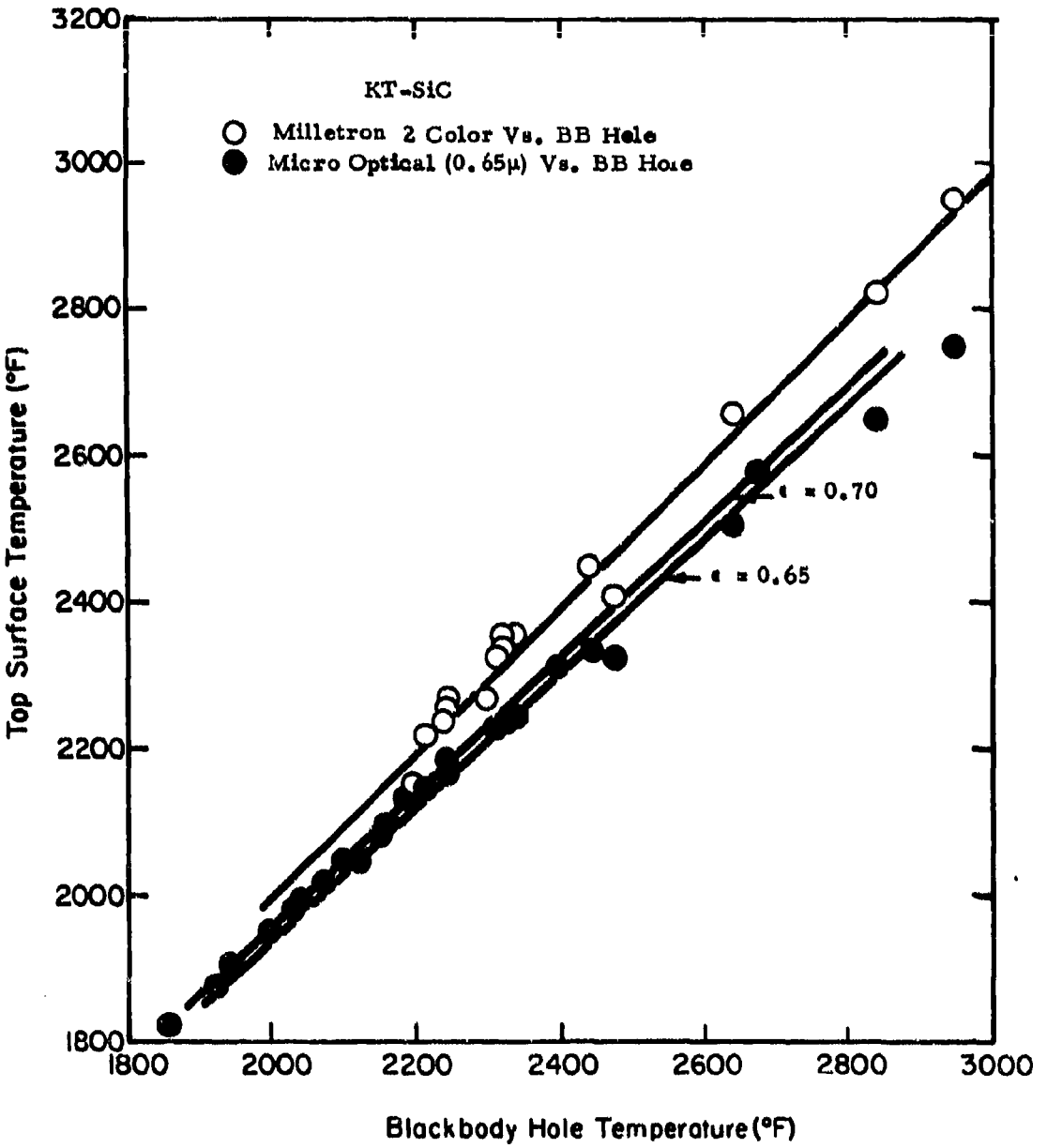

Figure 20. Temperature Gradients and Emittance of SiC in Static Air.

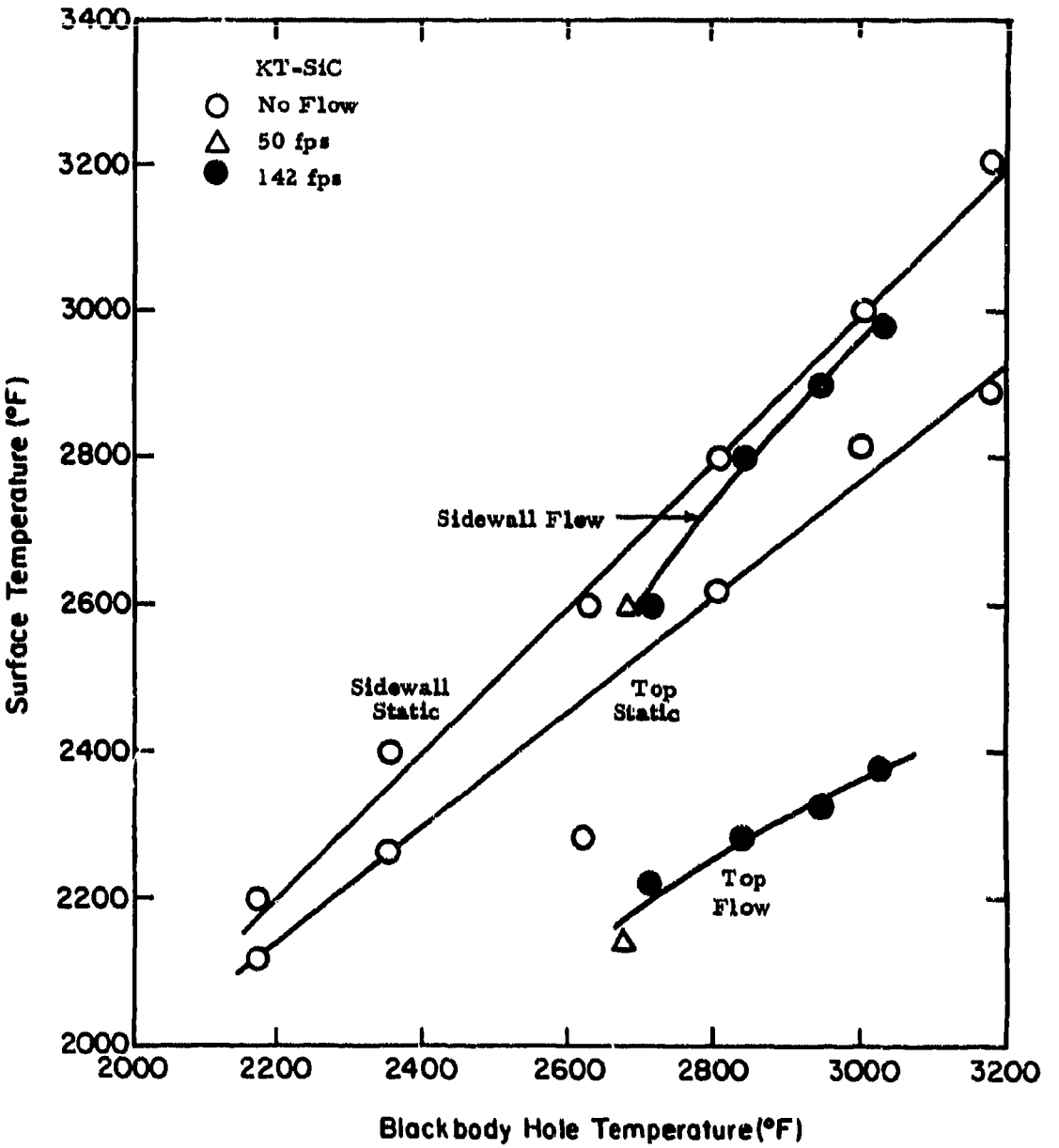

Figure 21. Effect of Flow on Temperature Gradients in SiC Cylinders.

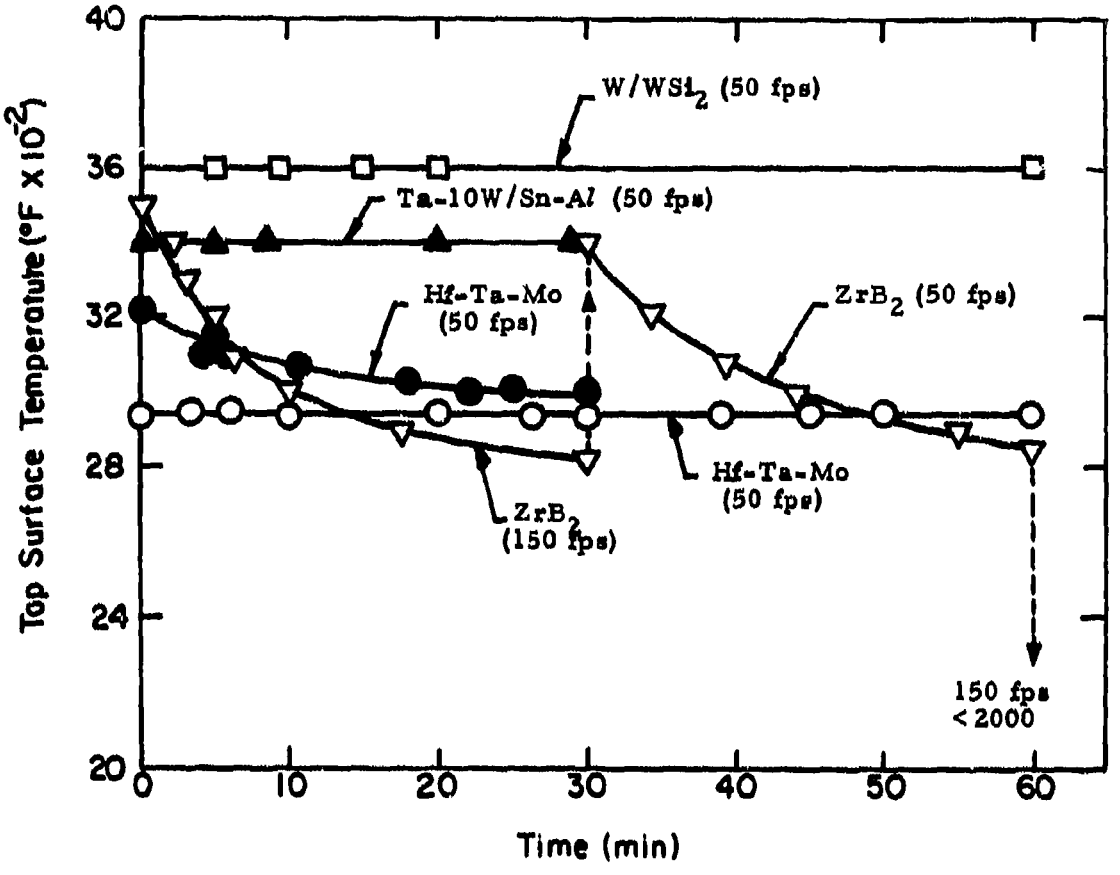

Figure 22. Effect of Holding Time and Gas Velocity on Test Temperature in CC/HW Flow Tests.

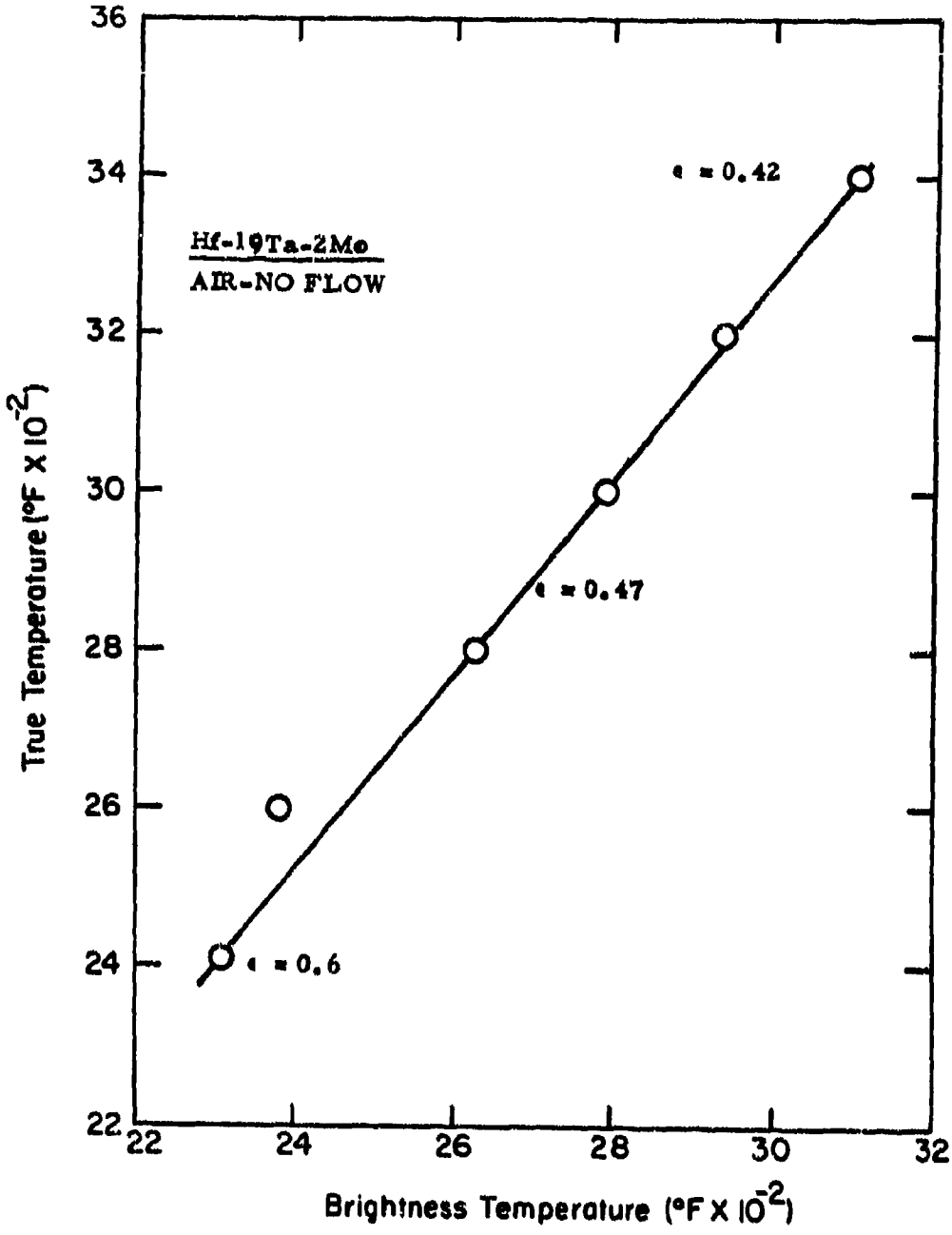

Figure 23. Emittance Calibration - Hf-Ta Alloy.

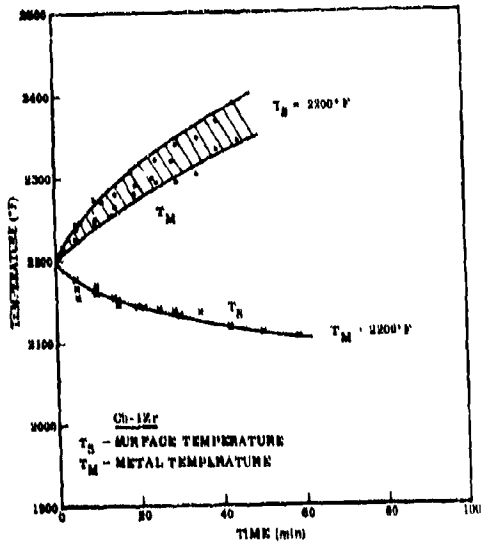

Figure 24. Temperature Drop through Cb_2O_5 Scale on Cb-1Zr.

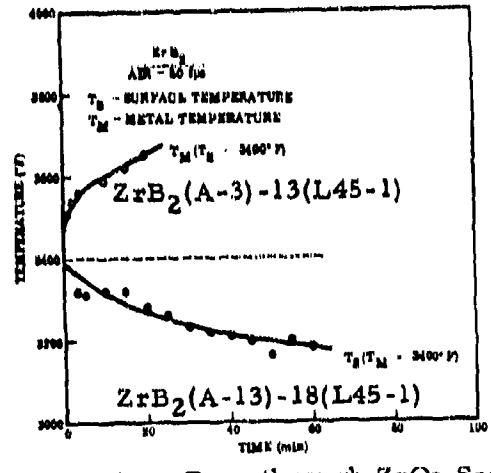

Figure 25. Temperature Drop through ZrO_2 Scale on ZrB_2.

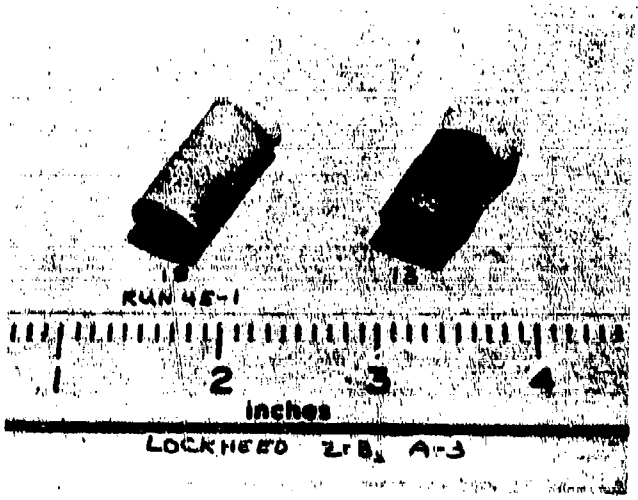

Plate No. 1-7116

Figure 26. Macrophotograph of ZrB_2(A-3)-18 (Lockheed 45-1) and ZrB_2(A-3)-13 (L46-1) after High Velocity CG/HW Exposure.

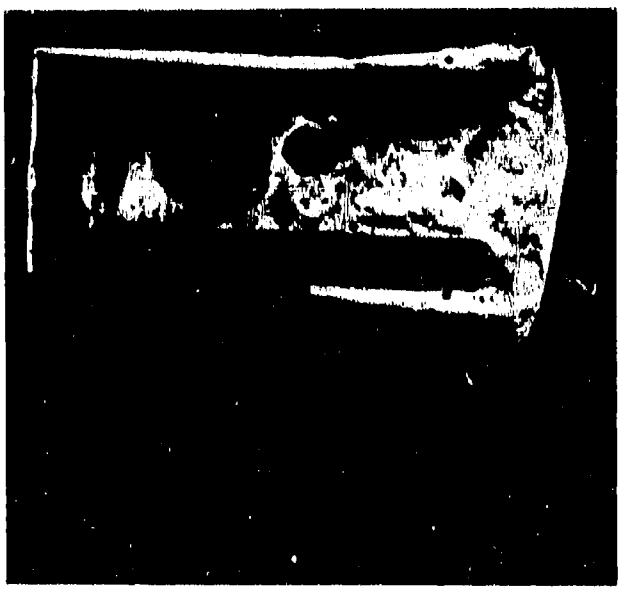

Plate No. 1-7117

As-Polished X2.75

Figure 27. Section Through ZrB_2(A-3)-13 (L46-1) after 30 Minute Exposure at 50 ft/sec in Air. Surface Temperature 3400°F. Top Surface at Left.

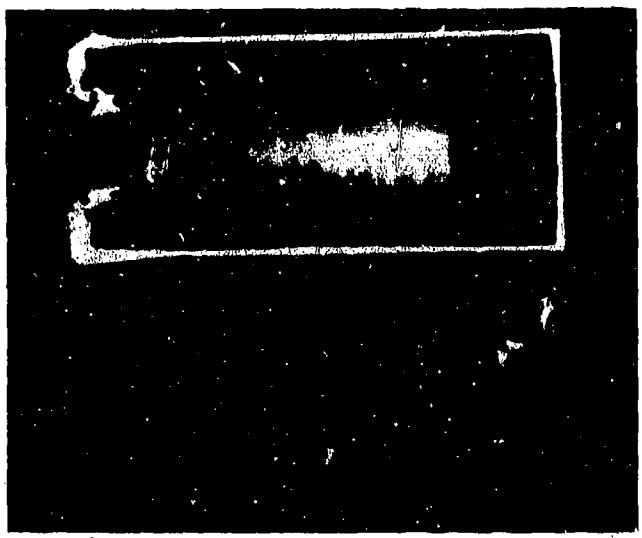

Plate No. 1-7120

As-Polished X2.63

Figure 28. Section Through ZrB_2(A-3)-18(L45-1) after 60 Minute Exposure at 50 ft/sec in Air. Substrate Temperature 3400°F.

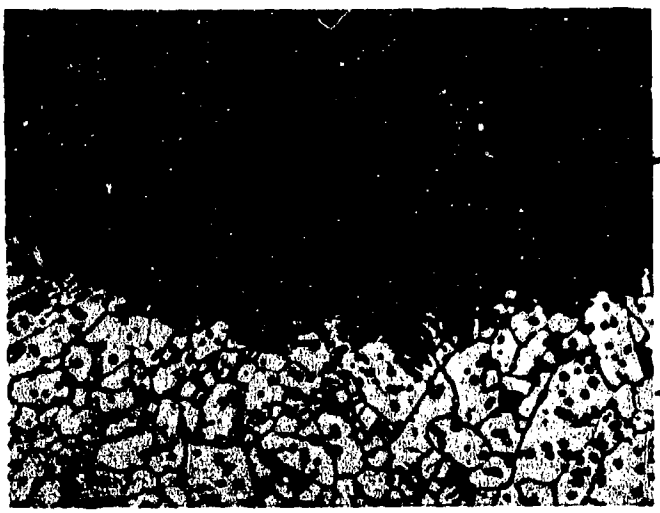

Plate No. 1-7123

Etched with 10 Glycerine $5HNO_3 3HF$ X250

Figure 29. Oxide-Matrix Interface of ZrB_2(A-3)-18(L45-1) Showing Adherent Oxide.

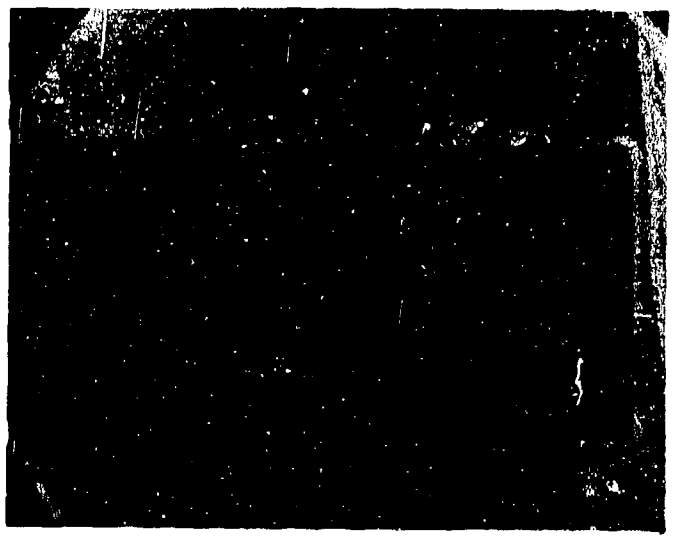

Plate No. 1-4830

As-Polished X3.5

Figure 30. Section through $HfB_{2.1}$(A-2)-13(L38-1) after 60 Minute Exposure at 50 ft/sec in CG/HW Test. Surface Temperature 3400°F. Oxide Thickness 8 Mils, Conversion Depth 4 Mils. Top Surface at Right.

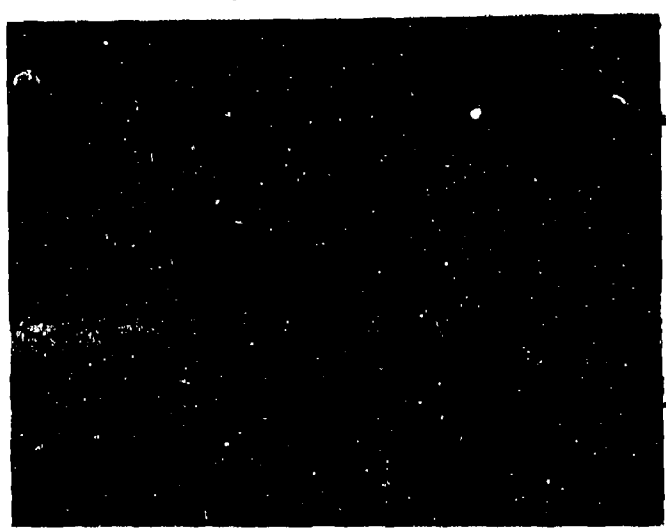

Plate No. 1-4831

Etched with 10 Glycerine 5$HNO_3$3HF X250

Figure 31. Oxide-Matrix Interface of $HfB_{2.1}$(A-2)-13 (L38-1) Showing Adherent Oxide. Oxide at Top.

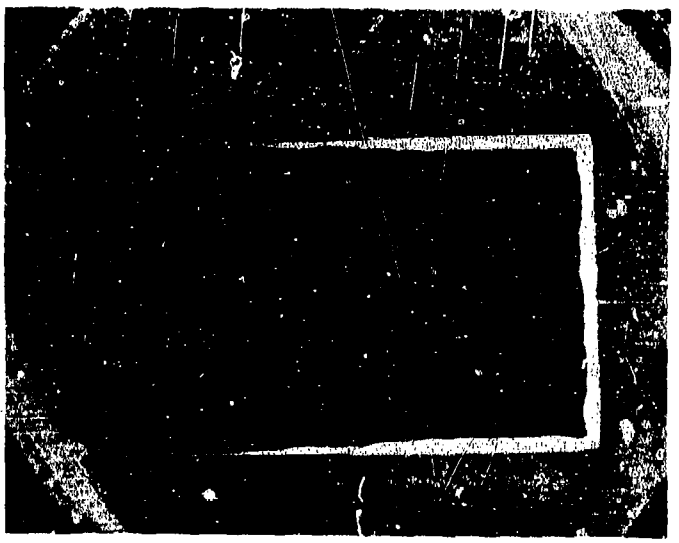

Plate No. 1-4833

As-Polished X3.5

Figure 32. Section Through $HfB_{2.1}$(A-2)-15(L39-2) after 60 Minute Exposure at 50 ft/sec in CG/HW Test. Surface Temperature 3600°-3190°F. Oxide Thickness 25 Mils. Conversion Depth 18 Mils Top Surface at Right.

Plate No. 1-4834

Etched with 10 Glycerine $5HNO_3 3HF$ X250

Figure 33. Oxide-Matrix Interface of $HfB_{2.1}$(A-3)-15 (L39-2) Showing Adherent Oxide.

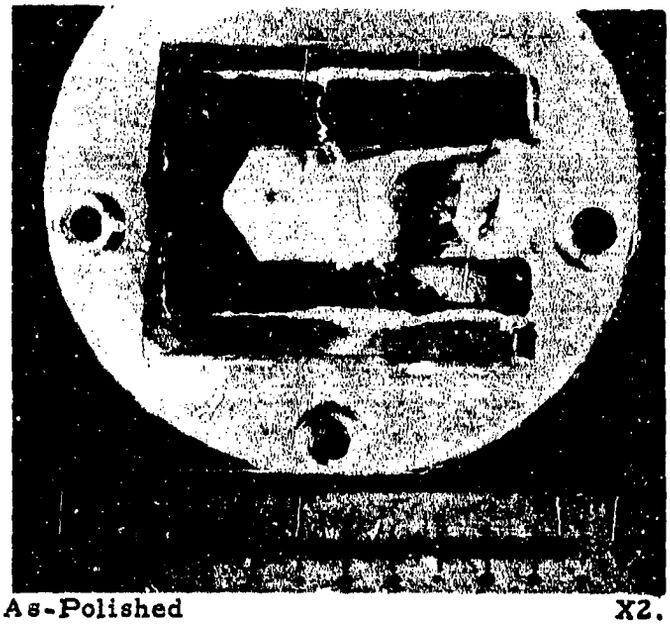

Plate No. 1-7142

As-Polished X2.69

Figure 34. Section Through Hf-19Ta-2Mo(I-23)(L44-1) after 30 Minutes at 1-10 ft/sec in CG/HW Test. Surface Temperature 3400°F. Sample Cracked after Test. Conversion Depth 14 Mils. Top Surface at Left.

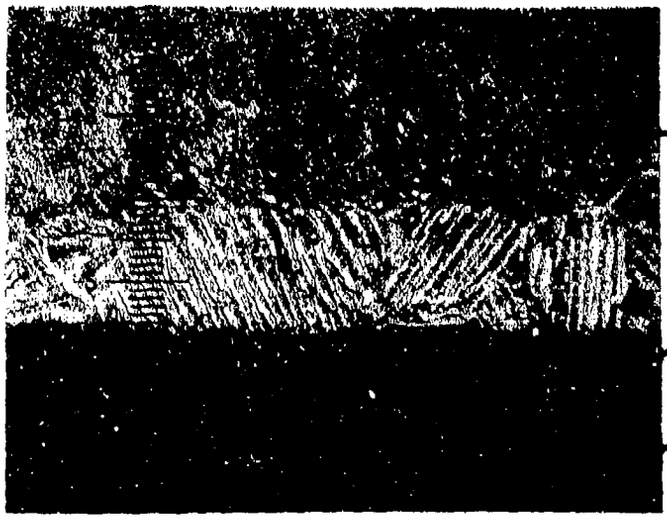

Plate No. -17599

Etched with 30 Lactic 10$HNO_3$1HF 0.788 mils/small division

Figure 35. Oxide-Subscale-Matrix Zones in Hf-19Ta-2Mo (I-23) (L44-1). Matrix at Top.

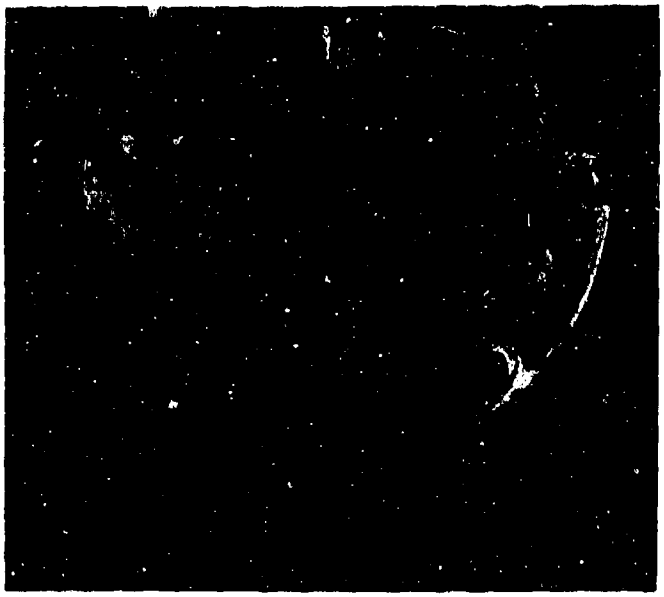

Plate No. 1-7146

As-Polished X2.62

Figure 36. Section Through Hf-19Ta-2Mo(I-23) (L44-2) after 60 Minutes at 1-10 ft/sec in CG/HW Test. Substrate Temperature 3355°F. Conversion Depth 12 Mils. Top Surface at Right.

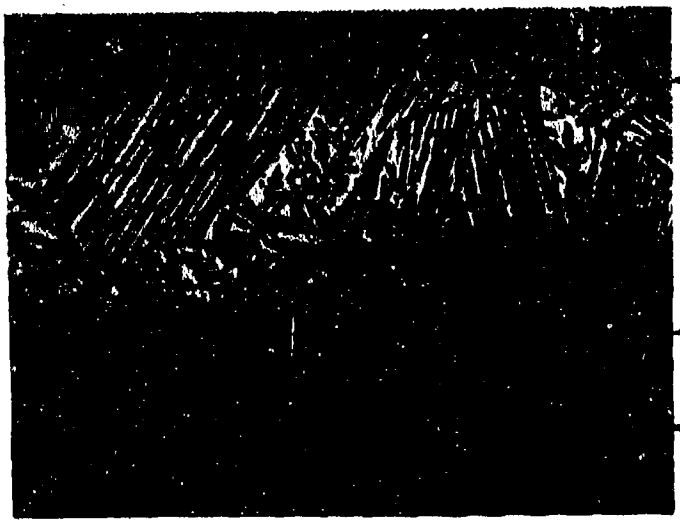

Plate No. 1-7600

Etched with 30 Lactic 10$HNO_3$1HF 0.788 mils/small division

Figure 37. Oxide-Subscale-Matrix Zones in Hf-19Ta-2Mo(I-23) (L44-2). Matrix at Top.

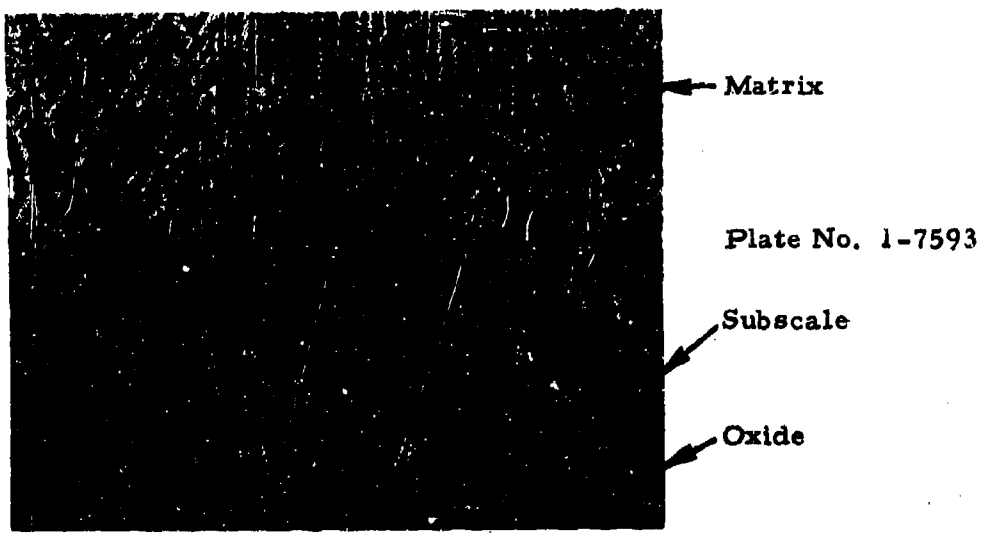

Etched with 30 Lactic 10$HNO_3$1HF 0.788 mils/small division

Figure 38. Oxide-Subscale-Matrix Interface of Hf-19Ta-2Mo(I-23) (L76-1) after 60 Minute Exposure at 50 ft/sec in CG/HW Test. Substrate Temperature 3500°F. Conversion Depth 20 Mils. Matrix at Top.

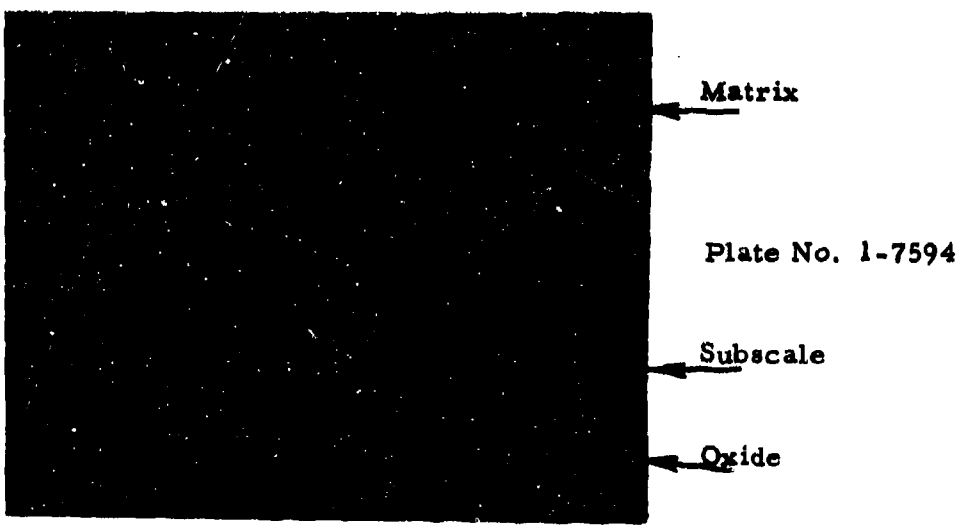

Etched with 30 Lactic 10$HNO_3$1HF 0.788 mils/small division

Figure 39. Oxide-Subscale-Matrix Interface of Hf-19Ta-2Mo (I-23) (L77-1) after 60 Minute Exposure at 50 ft/sec in CG/HW Test. Substrate Temperature 3700°F. Conversion Depth 31 Mils. Matrix at Top.

Plate No. 1-7137

As-Polished X2.78

Figure 40. Section through Hf-19Ta-2Mo (I-23) (L77-2) after 60 Minutes at 50 ft/sec in CG/HW Test. Substrate Temperature 3900°F. Conversion Depth 60 Mils. Top Surface at Right.

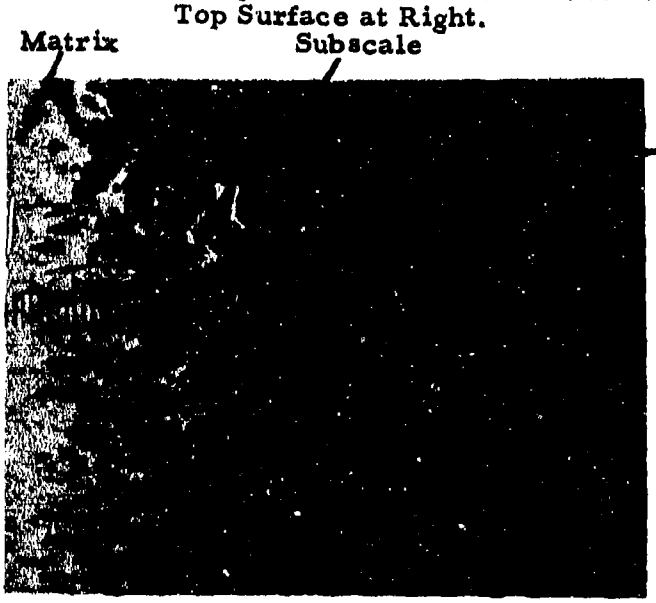

Plate No. 1-7595

Etched with 30 Lactic 10$HNO_3$1HF 0.788 mils/small division

Figure 41. Oxide-Subscale-Matrix Zones in Hf-19Ta-2Mo (I-23) (L77-2). Oxide at Right.

TABLE 1

TEST CAPABILITIES WITH THE LEPEL 475 KC - 23 KVA POWER SUPPLY

Maximum Top - Surface Temperature - °F

Velocity (fps)	KT-SiC[a,b]	KT-SiC[c]	Speer[d] Graphite	JTA	ZrB_2	Hf-19Ta-2Mo
1	>4000	4000	3850	3760	3610	3620
50	>4000	3290	3820	3700	3440	3240
75	>4000	3240	3780	3700	3300	3150
100	>4000	3210	3760	3600	3080	3090
125	>4000	3180	3740	3550	2820	3100
150	>4000	3140	3700	3450	2680	3100

a - Si-Rich, Hex.
b - Si-Lean, Cubic
c - Si-Lean, Hex.
d - Grade 710, 1.65 - 1.75 g/cc

TABLE 2

COMPARISON OF TEST CAPABILITIES WITH LEPEL (475 KC) AND TOCCO (10 KC) INDUCTION HEATING SOURCES

Maximum Top Surface Temperature - °F

Air Velocity (fps)	Hf-19Ta-2Mo		ZrB_2	
	Lepel	Tocco	Lepel	Tocco
1	3620	3400	3610	>3400
50	3240	3180	3440	-----
75	3150	3080	3300	-----
100	3090	3020	3080	-----
125	3100	2980	2820	-----
150	3100	2950	2680	3200
200		2800		

UNCLASSIFIED
Security Classification

DOCUMENT CONTROL DATA - R & D

(Security classification of title, body of abstract and indexing annotation must be entered when the overall report is classified)

1. ORIGINATING ACTIVITY (Corporate author)	2a. REPORT SECURITY CLASSIFICATION
ManLabs, Inc. 21 Erie Street Cambridge, Massachusetts 02139	UNCLASSIFIED 2b. GROUP N/A

3. REPORT TITLE

Stability Characterization of Refractory Materials Under High Velocity Atmospheric Flight Conditions - Part II, Volume II: Facilities and Techniques Employed for Cold Gas/Hot Wall Tests

4. DESCRIPTIVE NOTES (Type of report and inclusive dates)

Technical Documentary Report, April 1966 to July 1969

5. AUTHOR(S) (First name, middle initial, last name)

Larry Kaufman and Harvey Nesor

6. REPORT DATE	7a. TOTAL NO. OF PAGES	7b. NO. OF REFS
December 1969	55	8

8a. CONTRACT OR GRANT NO.	9a. ORIGINATOR'S REPORT NUMBER(S)
AF33(615)-3859	
b. PROJECT NO. 7312 Task 731201	N/A
c. 7350 Tasks 735001 and 735002	9b. OTHER REPORT NO(S) (Any other numbers that may be assigned this report)
d.	AFML-TR-69-84, Part II, Volume II

10. DISTRIBUTION STATEMENT This document is subject to export controls and each transmittal to foreign governments or foreign nationals may be made only with prior approval of the Air Force Materials Laboratory (MAMC), Wright-Patterson Air Force Base, Ohio 45433

11. SUPPLEMENTARY NOTES	12. SPONSORING MILITARY ACTIVITY
N/A	Air Force Materials Laboratory (MAMC) Wright-Patterson Air Force Base Ohio 45433

13. ABSTRACT

The oxidation of refractory borides, graphites and JT composites, hypereutectic carbide-graphite composites, refractory metals, coated refractory metals, metal oxide composites, and iridium coated graphites in air over a wide range of conditions was investigated over the spectrum of conditions encountered during reentry or high velocity atmospheric flight as well as those employed in conventional furnace tests. Elucidation of the relationship between hot gas/cold wall (HG/CW) and cold gas/hot wall (CG/HW) surface effects in terms of heat and mass transfer rates at high temperatures is a principal goal. The present report deals with facilities and techniques employed for performing low velocity CG/HW tests. These techniques include low velocity tests in resistance heated tube furnaces, low-velocity tests of inductively heated samples, and high velocity tests of inductively heated samples. Oxidation exposures performed by these techniques span the temperature range between 1000° and 4200°F at flow rates between 0.2 ft/sec and 300 ft/sec. Measurements of the temperature gradients through thin oxide films (10-60 mils thick) indicate that large differences up to 800°F are noted near 3500°F. These results have special significance with regard to interpretation of oxidation measurements and behavior.

This abstract is subject to special export controls and each transmittal to foreign governments or foreign nationals may be made only with prior approval of the Air Force Materials Laboratory (MAMC), W-PAFB, Ohio 45433

DD FORM 1 NOV 65 1473 REPLACES DD FORM 1473, 1 JAN 64, WHICH IS OBSOLETE FOR ARMY USE.

UNCLASSIFIED
Security Classification

UNCLASSIFIED
Security Classification

14. KEY WORDS	LINK A		LINK B		LINK C	
	ROLE	WT	ROLE	WT	ROLE	WT
Oxidation						
Refractory borides						
Graphites						
Composites						
Hypereutectic carbide-graphite composites						
Refractory metals						
Coated refractory metals						
Metal oxide composites						
Iridium coated graphites						
Facilities						
Techniques						
Low velocity tests						
Temperature gradients						

UNCLASSIFIED
Security Classification